Primary Intra-Axial Brain Tumours

13

Laura Oleaga, Javier Moreno, Mariano Werner, and Nuria Bargalló

13.1 Case 1

25-year-old female with a prior medical history of seizures non-responding to treatment.

Biopsy was performed; the pathological diagnosis was diffuse astrocytoma WHO grade II. Molecular and genetic features: isocitrate dehydrogenase (IDH1)-mutant, 1p/19q non-codeleted, and loss of ATRX expression, PFAG positive expression and P53 positive.

13.1.1 Images and Legends

L. Oleaga (✉) · J. Moreno · M. Werner · N. Bargalló
Radiology Department, Hospital Clínic Barcelona, Barcelona, Spain

Y. Özsunar, U. Şenol (eds.), *Atlas of Clinical Cases on Brain Tumor Imaging*,
https://doi.org/10.1007/978-3-030-23273-3_13

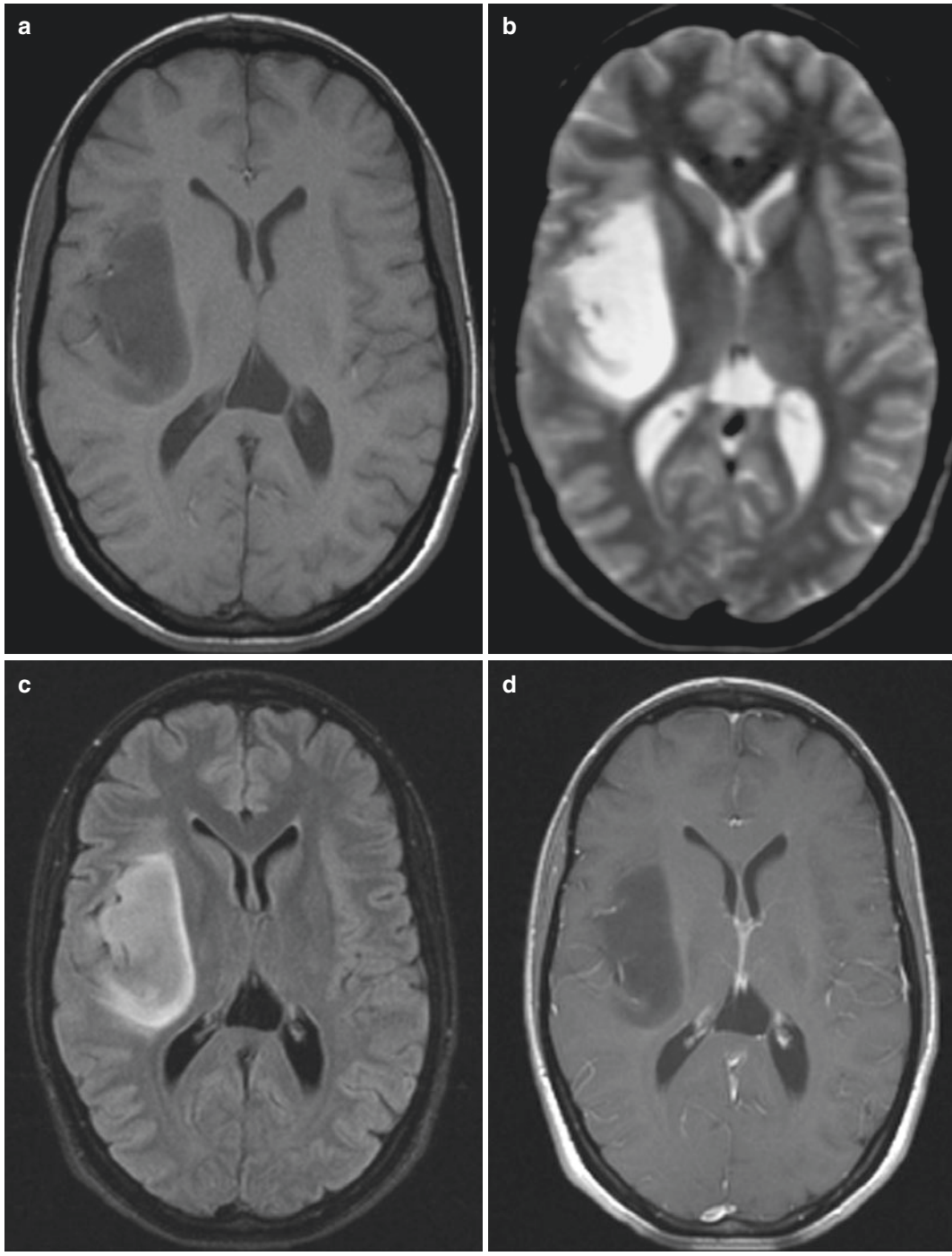

Fig. 13.1 (**a**) Axial T1-weighted MRI demonstrates low-signal intensity, well-defined mass on the right insular lobe. (**b**) 3D Sagittal T2-weighted MRI-axial reconstruction. Markedly T2-hyperintense right insular mass, similar to cerebrospinal fluid (CSF). (**c**) Axial FLAIR MRI, on this sequence the central part of the tumour, demonstrates substantially lower signal than the T2-weighted image (FLAIR/T2 mismatch). (**d**) Contrast-enhanced axial T1-weighted image demonstrates a well-defined non-enhancing insular mass. (**e**)Axial diffusion-weighted magnetic resonance imaging (DWI). Low signal is depicted on the tumour. (**f**) Apparent diffusion coefficient map (ADC). The tumour exhibits high ADC value. (**g**) Dynamic susceptibility contrast-enhanced MR image. Relative cerebral blood volume (rCBV) colour map shows a low rCBV, in keeping with a low-grade glioma. (**h**) ^{1}H-MR spectroscopy (TE 30 ms) shows a slightly elevated choline (Ch) peak with a diminished peak of N-acetyl aspartate (NAA) and increased myo-inositol (mIns)

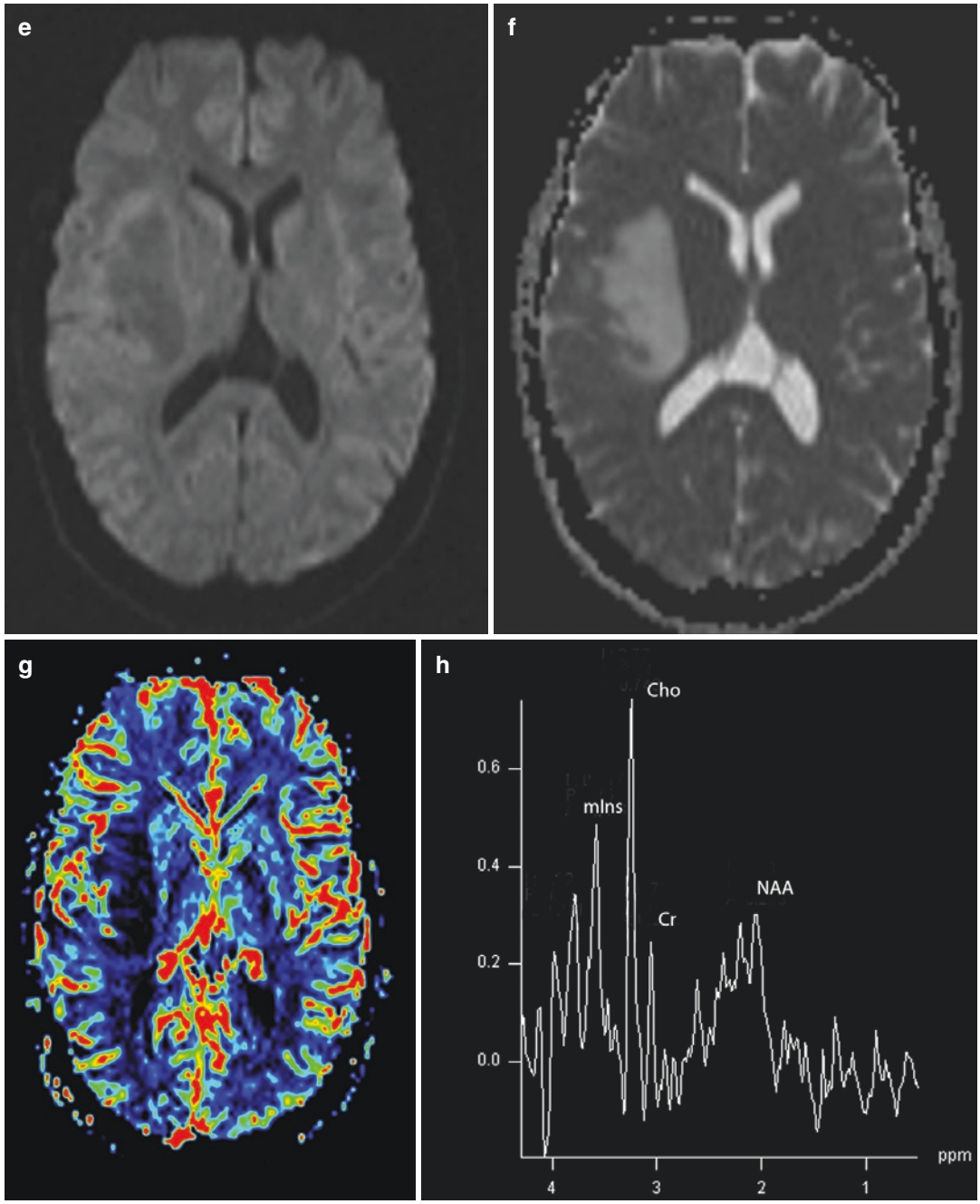

Fig. 13.1 (continued)

13.1.2 Epidemiology

Diffuse astrocytoma, IDH-mutant, are the most common WHO grade II astrocytomas.

13.1.3 Pathology and Genetics

The World Health Organization (WHO) has recently updated the diagnostic criteria for astrocytic and oligodendroglial tumours. Under the

new classification system, the diagnosis of diffuse glioma incorporates the mutation in the isocitrate dehydrogenase (IDH) genes, either type 1 (IDH1) or type 2 (IDH2) and simultaneous deletion of chromosomes 1p and 19q.

Maximum surgical resection, as feasible, is considered the best initial treatment option for WHO grade II astrocytomas (1p/19q non-codeleted). In cases of biopsy or incomplete resection, involved field radiotherapy and maintenance procarbazine, lomustine, and vincristine chemotherapy (RTOG 9802 trial) is recommended according to the European Association for Neuro-Oncology (EANO) guideline 2017.

13.1.4 Clinical Management

Molecular diagnostic tests are essential to select the appropriate treatment. Standard of care for WHO grade II astrocytomas IDH-mutant (1p/19q-non-codeleted) includes resection, as feasible, or biopsy followed by involved field radiotherapy and maintenance procarbazine, lomustine, and vincristine chemotherapy.

13.1.5 Imaging Findings and Differential Diagnosis

MR imaging feature labelled "T2-FLAIR mismatch" has been demonstrated in diffuse astrocytoma IDH-mutant 1p/19q non-codeleted. The lack of enhancement on the conventional MR image suggests a low-grade glioma.

rCBV measurements correlate with tumour grade and histologic findings of increased vascularity. Astrocytic low-grade tumours show low rCBV values.

ADC maps can also be used as grade tumour predictors. DWI quantifies the water diffusivity within the intra- and extracellular compartments, there is an inverse correlation between the minimum ADC values and histopathologic grade of the astrocytic supratentorial brain tumours. Low-grade tumours show low diffusivity and high ADC values.

Take-Home Messages

- The presence of >50% T2-FLAIR mismatch is highly predictive of a IDH-mutant 1p/19q non-codeleted tumour

Further Reading

1. Johnson DR, Guerin JB, Giannini C, Morris JM, Eckel LJ, Kaufmann TJ. 2016 Updates to the WHO Brain Tumor Classification System: What the Radiologist needs to know. RadioGraphics 2017; 37:2164–2180
2. Lasocki A, Gaillard F, Gorelik A, Gonzales M. MRI features can predict 1p/19q status in intracranial gliomas. Am J Neuroradiol. 2018; 39:687–692
3. Patel SH, Poisson LM, Brat DJ, Zhou Y, Cooper L, Snuderl M, Thomas C, Franceschi AM, Golfinos JG, Chi AS, Jain R. T2–FLAIR mismatch, an imaging biomarker for IDH and 1p/19q status in lower-grade gliomas: A TCGA/TCIA Project. Clin Cancer Res. 2017; 23:6078–6085
4. Broen MPG, Smits M, Wijnenga MMJ, Dubbink HJ, Anten MHME, Schijns OEMG, Beckervordersandforth J, Postma AA, van den Bent MJ. The T2–FLAIR mismatch sign as an imaging marker for non-Enhancing IDH-mutant, 1p/19q-intact lower grade glioma: a validation study. Neuro Oncol. 2018;3(20):1393–1399
5. Leu K, Ott GA, Lai A, Nghiemphu PL, Pope WB, Yong WH, Liau LM, Cloughesy TF, Ellingson BM. Perfusion and diffusion MRI signatures in histologic and genetic subtypes of WHO grade II–III diffuse gliomas. J Neurooncol 2017; 134:177–188

13.2 Case 2

35-year-old female, with a sudden loss of consciousness, prior history of hemiparesis and multiple cranial nerve palsies with a clinical suspicion of multiples sclerosis (MS). Steroid treatment was started with symptoms worsening.

Biopsy was performed; the pathological diagnosis was diffuse astrocytoma WHO II, negative isocitrate dehydrogenase (IDH) wild-type, 1p19q non-codeleted, loss of ATRX expression, PFAG positive expression and P53 positive. The tumour shows high proliferation index Ki67 17%.

The patient was treated with temozolamide and radiation therapy.

13.2.1 Images and Legends

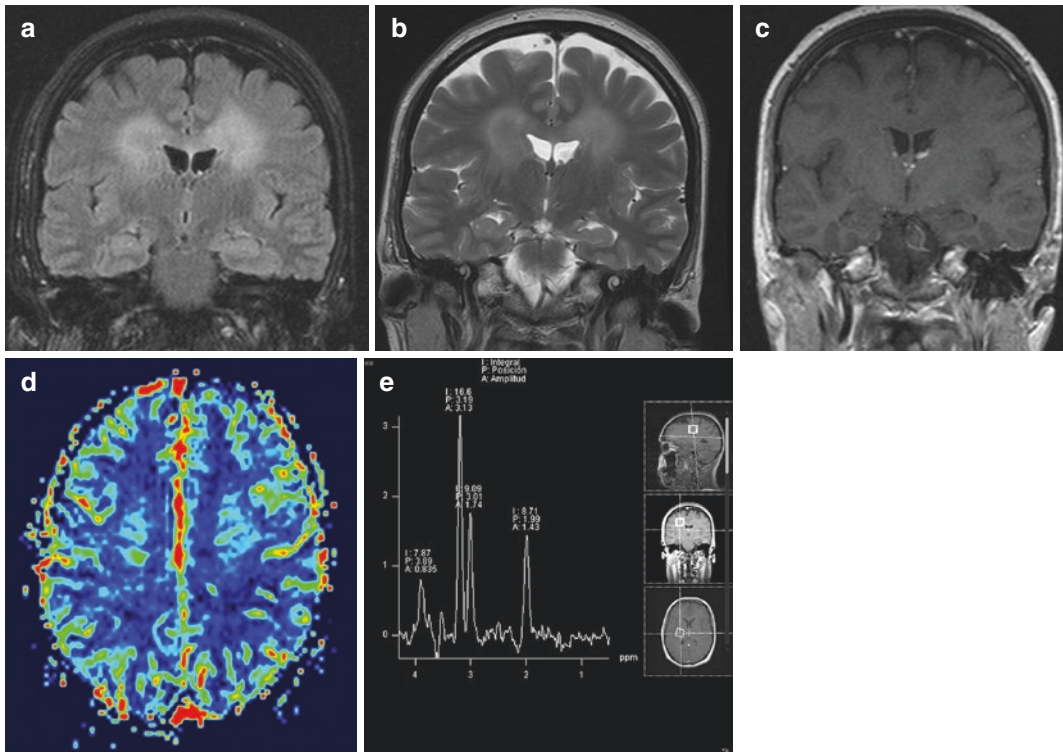

Fig. 13.2 (**a**) Coronal T2 FLAIR MRI demonstrates an ill-defined mass in both centrum semiovale with corpus callosum infiltration. (**b**) Coronal T2-weighted MRI. Slight mass effect of the lesion is shown. U-fibbers are spared. No mismatch on FLAIR images is demonstrated. (**c**) Coronal T1-weighted MRI post-Gd administration shows no enhancement whatsoever. (**d**) Dynamic susceptibility contrast-enhanced MR image. Relative cerebral blood volume (rCBV) colour map shows slight increase of perfusion possibly secondary to the high cellularity of the lesion. A possible pitfall may be the transcortical veins at this region. (**e**) MR spectroscopy shows a slightly elevated choline peak associated with a diminished peak of N-acetyl aspartate (NAA)

13.2.2 Epidemiology

Diffuse astrocytomas are tumours diagnosed in childhood or young adulthood (biphasic distribution 6–12 years and 26–46 years).

13.2.3 Pathology and Genetics

According to the new WHO 2016 classification of CNS tumours, there are three variants of diffuse astrocytoma: IDH-mutant, IDH no mutant (wild type) and NOS (no otherwise specified). Diffuse astrocytomas, IDH-wild type with no 1p19q codeletion, are the most aggressive grade II astrocytomas.

13.2.4 Clinical Management

Maximum surgical resection, as feasible, is considered the best initial treatment option for WHO grade II astrocytomas (1p/19q non-codeleted). In cases of biopsy or incomplete resection, involved field radiotherapy and temozolamide is recommended according to the European Association for Neuro-Oncology (EANO) guideline 2017.

13.2.5 Imaging Findings and Differential Diagnosis

Wild-type diffuse astrocytoma is usually a mass-like hyperintense on T2-weighted images, non-enhancing lesion, which follows white matter distribution. Cortical involvement is possible in late cases. In comparison with the IDH-mutant, the borders of the wild type are usually ill defined; also the FLAIR mismatch is absent. rCBV measurements correlate with tumour grade and histologic findings of increased vascularity. Astrocytic low-grade tumours show low rCBV values. High cellular tumours show high rCBV values.

Take-Home Messages

- Wild-type DA is usually a smaller lesion with ill-defined border in comparison with the more benign IDH-mutant DA

Further Reading

1. Louis DN, Perry A, Reifenberger G et al. The 2016 World Health Organization Classification of Tumors of the Central Nervous System: a summary. Acta Neuropathol. 2016; 131: 803–20
2. Patel SH, Poisson LM, Brat DJ, Zhou Y, Cooper L, Snuderl M, Thomas C, Franceschi AM. et al. T2–FLAIR mismatch, an imaging biomarker for IDH and 1p/19q status in lower-grade gliomas: A TCGA/TCIA project. Clin Cancer Res. 2017; 23:6078–6085
3. Brat DJ, Verhaak RG et al. Comprehensive, integrative genomic analysis of diffuse lower-grade gliomas. N. Engl. J. Med. 2015; 372: 2481–2498
4. Lasocki A, Gaillard F, Gorelik A, Gonzales M. MRI features can predict 1p/19q status in intracranial gliomas. Am J Neuroradiol. 2018; 39:687–692

13.3 Case 3

64-year-old male presents with first episode of seizures. The patient was previously asymptomatic.

The patient underwent complete surgical resection of the temporal mass. Biopsy was performed and pathology showed histologic features of glioblastoma (GB). The patient received TMZ + RDT according to Stupp Protocol. Four years later, the patient developed a right frontal superficial nodule. Surgical resection was performed. Pathology of the second lesion showed a conventional GB with meningeal infiltration and a region with cystic areas and small blue cells with positive synaptophysin. Final diagnosis was GB with primitive neuroectodermal tumour (PNET)-like component. There was no PNET component in the first pathology specimen.

13.3.1 Images and Legends

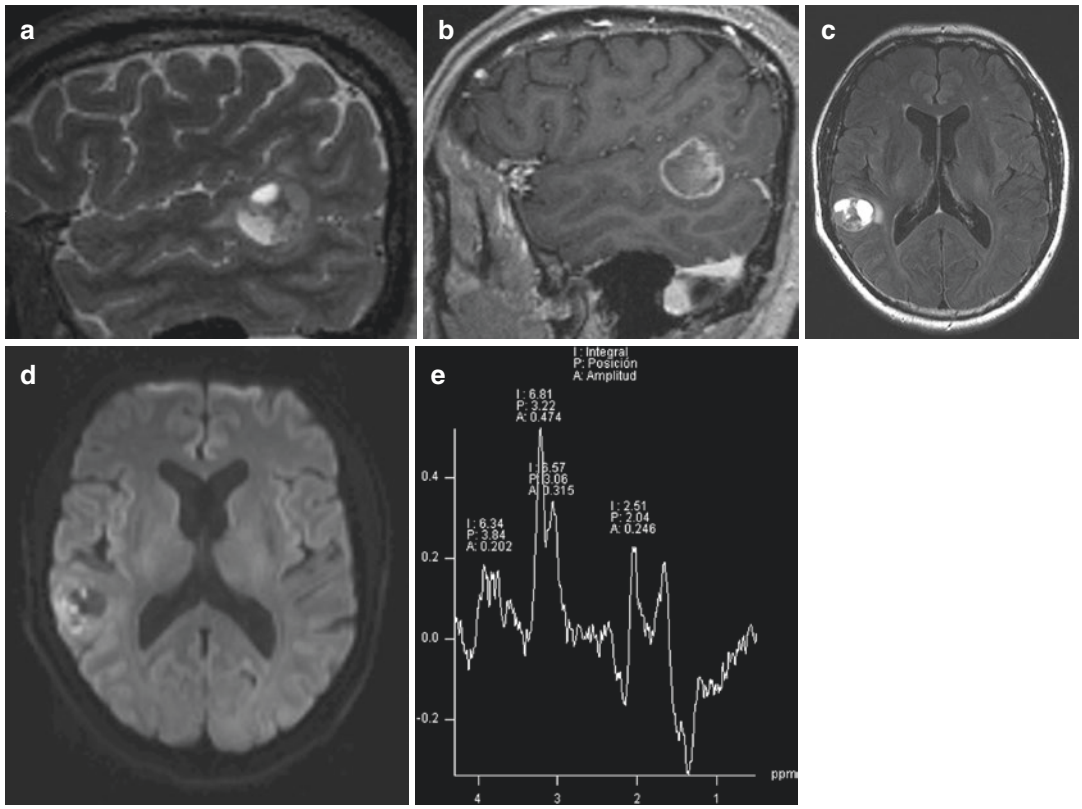

Fig. 13.3 (**a**) T2W 3D SPACE MRI. Right cortical tumour with anterior cystic and solid areas. (**b**) T1GRE 3D+Gd MRI. Enhancement of the solid part of the tumour and a peripheral enhancing rim. (**c**) T2 FLAIR MRI shows a rim of peripheral hyperintense oedema in adjacent white matter. (**d**) DWI MRI. The posterior nodular part of the lesion shows a hypercellular zone with high diffusion. (**e**) ^{1}H-MR spectroscopy (TE 30 ms) shows a Choline peak and reduction of the NAA

13.3.2 Epidemiology

GB with PNET-like components is a rare variant of GB. There is an increased propensity of these tumours for CSF dissemination and a benefit of "PNET-like" chemotherapy.

13.3.3 Pathology, Imaging and Genetics

GB with PNET component has two areas with different histological architectures:

The traditional astrocytic GB areas with high expression of GFA, 10q deletion, EGFR amplification and 1p/19q deletions. IDH mutations are variable. MR signal is very variable hence the name "multiforme". Enhancement and necrosis are common with an ill-defined lesion and severe mass effect. rCBV measurements are elevated in the viable tumour areas.

Hypercellular undifferentiated PNET areas, present lower expression of GFAP and variable neuronal immunophenotype (S-100, synaptophysin, NeuN, NSE and NFP). Also high Ki-67 index, N-myc or C-myc amplifications are reported. MR aspect of the region features cystic areas and high restriction (secondary to the high cellularity of the lesion).

GB-PNET tumours feature behaviour from both histologic regions, GB-PNET tumour tends to disseminate to CSF and has fewer local recurrence in comparison with conventional GB.

13.3.4 Clinical Management

There is no consensus with treatment; most series has been treated with TMZ and local RDT. There are some reports with possible benefit of carboplatin and whole spine RDT for reducing CSF dissemination.

Take-Home Messages

- GB-PNET lesions present both MR characteristics and behaviour from both histologic origins of the tumour. High restriction and CSF spread are some specific aspect of the tumour. Lower local recurrence rates are reported

Further Reading

1. Louis DN, Perry A, Reifenberger G et al. The 2016 World Health Organization Classification of Tumors of the Central Nervous System: a summary. Acta Neuropathol. 2016; 131: 803–820
2. Varlet P, Soni D, Miquel C, Roux FX, Meder JF, Chneiweiss H, Daumas-Duport C. New variants of malignant glioneuronal tumors: a clinicopathological study of 40 cases. Neurosurgery. 2004; 55:1377–1391
3. Lee APS, Brewer J, Back M, Wheeler H. Combination therapy for glioblastoma multiforme with primitive neuroectodermal tumor components: case series. J Clin Oncol. 2012; 30(Suppl 15):e12507
4. Perry A, Miller CR, Gujrati M, Scheithauer BW, Zambrano SC, Jost SC, Raghavan R, Qian J, Cochran EJ, Huse JT, Holland EC. Malignant gliomas with primitive neuroectodermal tumor-like components: a clinicopathologic and genetic study of 53 cases. Brain Pathology. 2009; 19:81–90

13.4 Case 4

57-year-old male. Sudden-onset of aphasia and vomiting. Biopsy was performed; the pathological diagnosis was GB, WHO grade IV, negative for ATRX, p53, IDH1 (wild-type) and IDH2. No MGMT hypermethylation is noted. High expression of EGFR is demonstrated.

The patient was treated with TMZ + RT. 8 months later the patient presented with severe progression of the disease with cranial hypertension, neurological deterioration and pneumonia. The patient died 9 months later.

13.4.1 Images and Legends

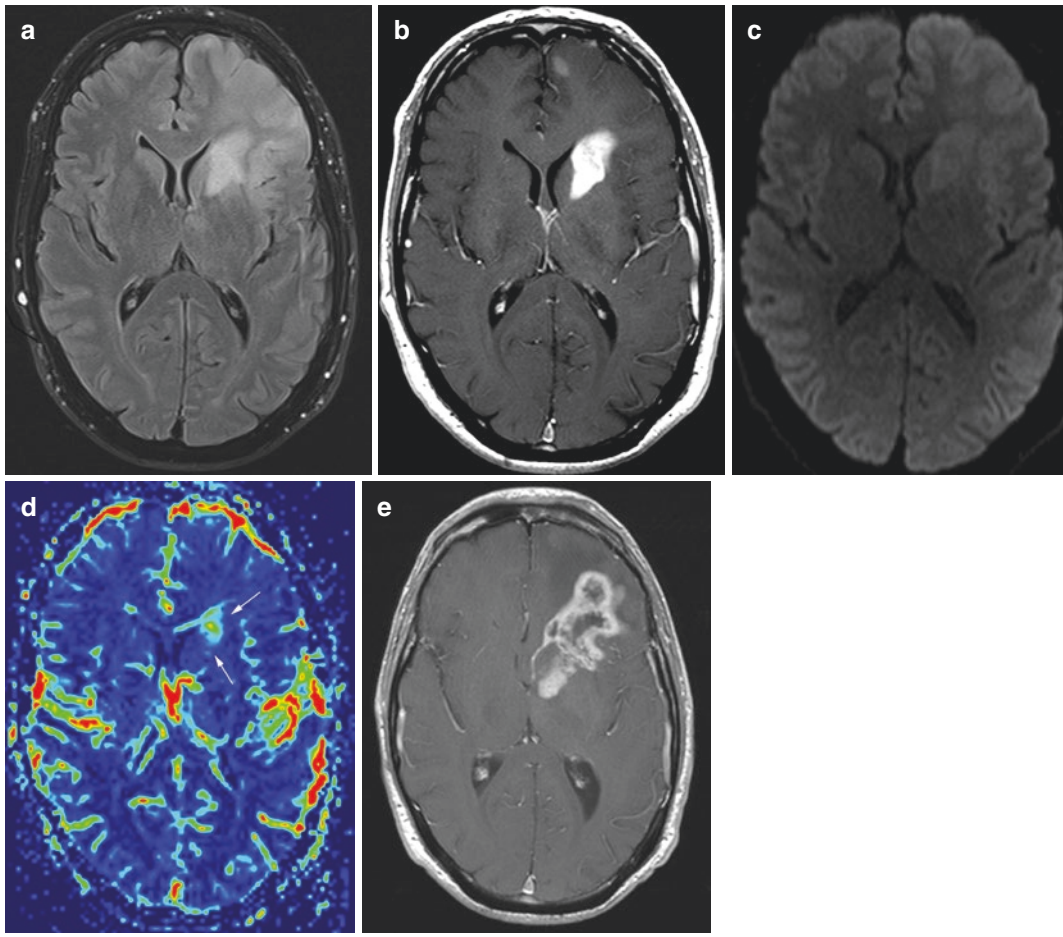

Fig. 13.4 (**a**) Axial FLAIR MRI. Left frontal mass involving the cortex and corona radiata. (**b**) Axial T1W + Gd MRI. Nodular deep enhancement is demonstrated with some foci in the sub-cortical areas. (**c**) Dynamic susceptibility contrast-enhanced MR image. Relative cerebral blood volume (rCBV) colour map shows increased rCBV (arrows) in the enhancing region. (**d**) DWI MRI. The mass shows slightly increased signal in keeping with hypercellular tumour. (**e**) 8 months follow-up MRI T1SE + Gd. Massive progression of the mass is noted with midline crossing at the callosum (butterfly lesion) and necrotic areas. Ependymal spread is noted in the frontal horn of the ventricle

13.4.2 Epidemiology

GB is a tumour with a global incidence of less than 10/100.000 people. GB accounts for 50% of all gliomas. It has a poor prognosis of 15 months survival rate.

13.4.3 Pathology and Genetics

Glioblastoma is the most aggressive, invasive and undifferentiated type astrocytic of tumour and has been designated Grade IV by WHO. According to the origin, 90% of the GBs are primary type, also known as "wild type" (without IDH mutation or MGMT methylation). Secondary GB is IDH mutated and arises from a previous low-grade glioma. Wild-type GB shows a typical EGFR amplification and aggressive behaviour.

13.4.4 Clinical Management

Surgical debulking or total excision + temozolomide and radiation therapy are the typical management of the lesion.

13.4.5 Imaging Findings and Differential Diagnosis

GB usually shows an extensive supratentorial lesion with variable enhancement (always present, although) with signs of hypercellularity and necrosis. Butterfly image is frequent. At the moment of diagnosis, some signs of extensive spread are more frequent on WT GBs, as ependymal or leptomeningeal spread. DWI and rCBV maps correlate with the histologic grade of the GBs.

Take-Home Messages

- Wild-type GBs are the most aggressive subtype of GB. They arise from a previous normal brain

Further Reading

1. Kumar V, Abbas AK, Fausto N et al. Robbins and Cotran pathologic basis of disease. W B Saunders Co. (2005) ISBN:0721601871
2. Rees JH, Smirniotopoulos JG, Jones RV et al. Glioblastoma multiforme: radiologic-pathologic correlation. Radiographics. 1996; 16: 1413–38
3. Omuro A, DeAngelis LM. Glioblastoma and other malignant gliomas: a clinical review. JAMA. 2013; 310:1842–1850
4. Osborn AG, Salzman KL, Jhaveri MD, Barkovich AJ. Diagnostic imaging: brain E-book. Elsevier Health Sciences; 2015 Dec 24
5. Lacroix M, Abi-Said D, Fourney DR, Gokaslan ZL, Shi W, DeMonte F, Lang FF, McCutcheon IE, Hassenbusch SJ, Holland E, Hess K. A multivariate analysis of 416 patients with glioblastoma multiforme: prognosis, extent of resection, and survival. Journal of neurosurgery. 2001; 95:190–198
6. Thakkar JP, Dolecek TA, Horbinski C, et al. Epidemiologic and molecular prognostic review of Glioblastoma. Cancer Epidemiol Biomarkers Prev. 2014; 23:1985–1985

13.5 Case 5

63-year-old man with headache, altered mental status and left-hand weakness from months ago.

Biopsy was performed; the pathological diagnosis was glioblastoma, WHO grade IV. Molecular and genetic features: isocitrate dehydrogenase (IDH1)-wild-type, methylguanine methyltransferase (MGMT) negative, P53 negative, EGFR negative, EGFRvIII negative. TERT mutation. c .–124C > T.

13.5.1 Images and Legends

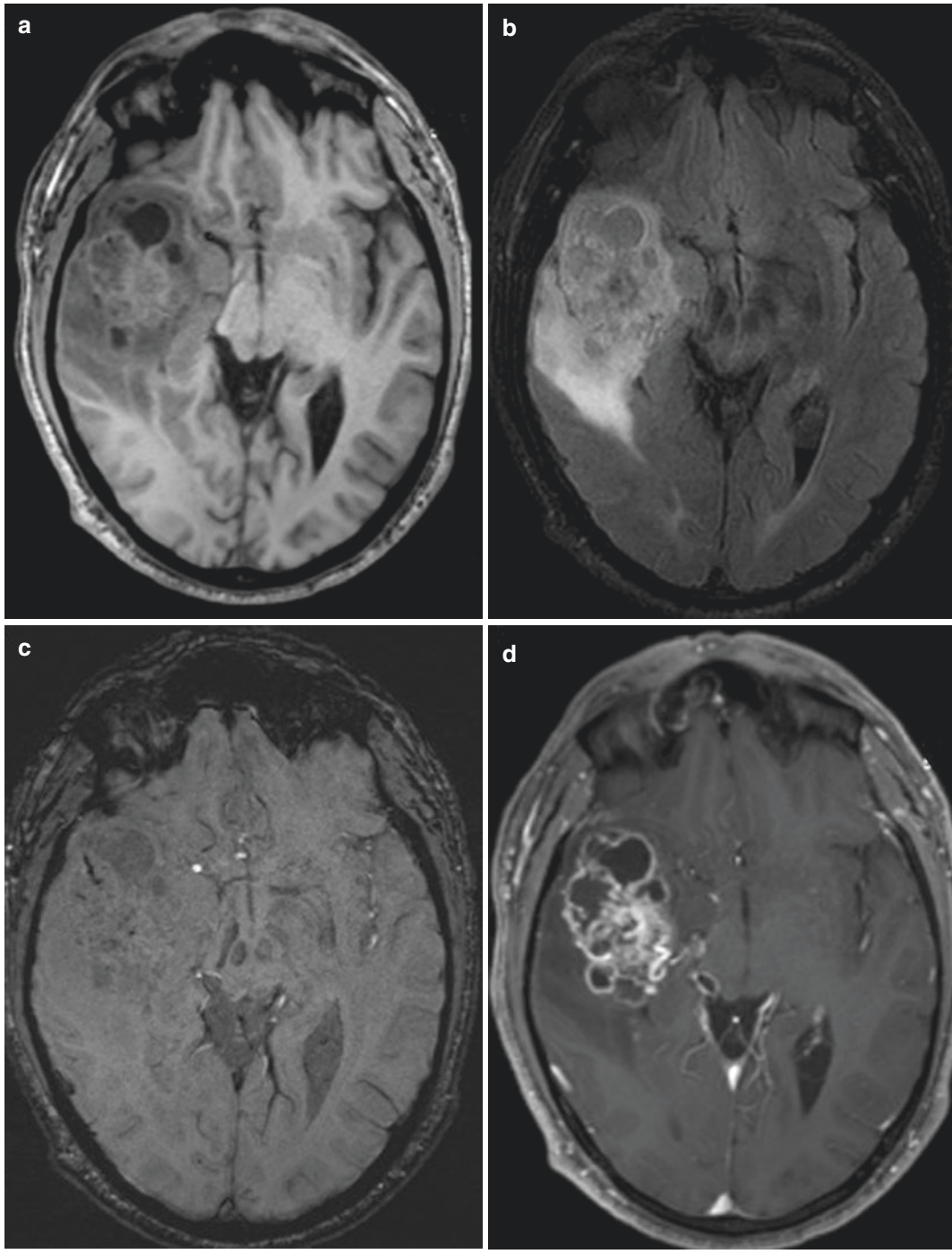

Fig. 13.5 (**a**) Axial T1-weighted MRI demonstrates a heterogeneous mass involving the temporo-insular region. (**b**) Axial FLAIR MRI shows hyperintense solid regions with central hypointense areas of necrosis surrounded by vasogenic oedema. (**c**) Axial SWI demonstrates susceptibility artefact inside the lesion due to presence of blood products. (**d**) Contrast-enhanced axial T1-weighted MRI demonstrates thick, irregular predominantly peripheral enhancement with central necrosis. (**e**) MR perfusion shows rCBV elevated in solid enhancing regions of the tumour. (**f**) DTI demonstrates high signal in solid parts related to hypercellularity. (**g**) Low ADC values correlated with high-grade gliomas

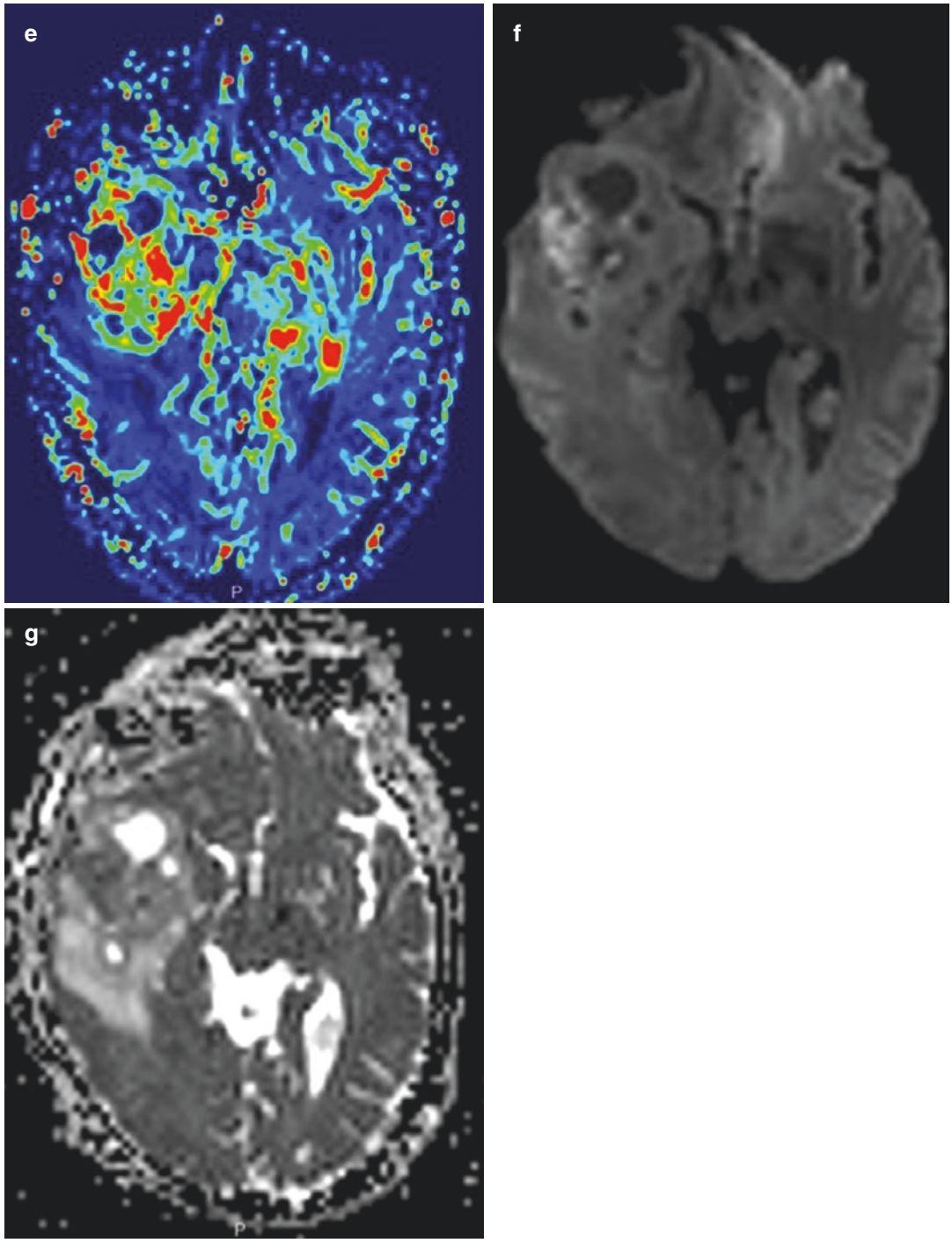

Fig. 13.5 (continued)

13.5.2 Epidemiology

There are two types of glioblastomas:

- Glioblastoma, IDH-wild type (90% of cases), which corresponds with the clinically defined primary glioblastoma and occurs in patients over 55 years of age
- Glioblastoma, IDH-mutant (10% of cases), which corresponds to secondary glioblastoma with a history of prior lower grade diffuse glioma and usually affect younger patients

13.5.3 Pathology and Genetics

- Glioblastoma, IDH-wild type. IDH negative, related to poor prognosis. MGMT methylation (60%). TERT promoter mutations (72%). TP53 mutations (27%). ATRX mutations (exceptional). EGFR amplification (35%). PTEN mutations (24%)
- Glioblastoma, IDH-mutant. IDH positive, related to better prognosis. MGMT methylation (80%). TERT promoter mutations (26%). TP53 mutations (81%). ATRX mutations (71%). EGFR amplification (exceptional). PTEN mutations (exceptional)

13.5.4 Clinical Management

After a complete surgical resection, the patient received standard treatment with temozolomide (TMZ) and radiation therapy.

The **Stupp protocol** (radiotherapy plus temozolomide) has become standard of care for the treatment of these patients since it has led to significant survival improvements.

13.5.5 Imaging Findings and Differential Diagnosis

Glioblastomas are usually seen as a heterogeneous enhancing mass. They tend to be hypointense in T1WI and hyperintense in T2/FLAIR surrounded by vasogenic oedema and may have susceptibility artefact on SWI from blood products. Lower ADC values in solid areas are related with high-grade tumours. They show heterogeneous enhancement on contrast images, irregular and predominantly peripheral. Perfusion images show increased rCBV in solid enhancing areas. MR spectroscopy demonstrates increased Choline, lactate and lipids and decreased NAA and myoinositol.

Differential diagnosis includes cerebral metastasis, primary CNS lymphoma, cerebral abscess and tumefactive demyelination.

Take-Home Messages

- Glioblastomas are heterogeneous enhancing intra-axial masses with poor prognosis despite treatment

Further Reading

1. Louis DN, Perry A, Reifenberger G, von Deimling A, Figarella-Branger D, Cavenee WK, et al. The 2016 World Health Organization Classification of Tumors of the Central Nervous System: a summary. Acta Neuropathol. Springer Berlin Heidelberg; 2016; 131:803–820
2. Stupp R, Mason WP, van den Beuf MJ. Radiotherapy plus concomitant and adjuvant temozolomide for newly diagnosed glioblastoma. N Engl J Med. 2005; 352: 987–96
3. Perry JR, Laperriere N, O'Callaghan CJ, Brandes AA, Menten J, Phillips C, et al. Short-Course Radiation plus Temozolomide in Elderly Patients with Glioblastoma. N Engl J Med 2017; 376:1027–1037
4. Yamashita K, Hiwatashi A, Togao O, Kikuchi K, Hatae R, Yoshimoto K, et al. MR Imaging – Based Analysis of Glioblastoma Multiforme: Estimation of IDH1 Mutation Status. AJNR 2016; 37:58–65
5. Krex D, Klink B, Hartmann C, Von Deimling A, Pietsch T, Simon M, et al. Long-term survival with glioblastoma multiforme. Brain. 2007;130:2596–2606
6. Hilario A, Ramos A, Perez-Nuñez A, Salvador E, Millan JM, Lagares A, et al. The added value of apparent diffusion coefficient to cerebral blood volume in the preoperative grading of diffuse gliomas. Am J Neuroradiol. 2012; 33:701–707

13.6 Case 6

66-year-old female with left facial pain and hypoesthesia, swelling in the left malar region and left retro-orbital pressure for a month.

Biopsy was performed; the pathological diagnosis was gliosarcoma, Ki67 40%, WHO grade IV. Molecular and genetic features: Isocitrate dehydrogenase (IDH1)-wild-type, Methylguanine methyltransferase (MGMT) promoter methylation, ATRX wild-type, P53 negative, EGFR negative.

13.6.1 Images and Legends

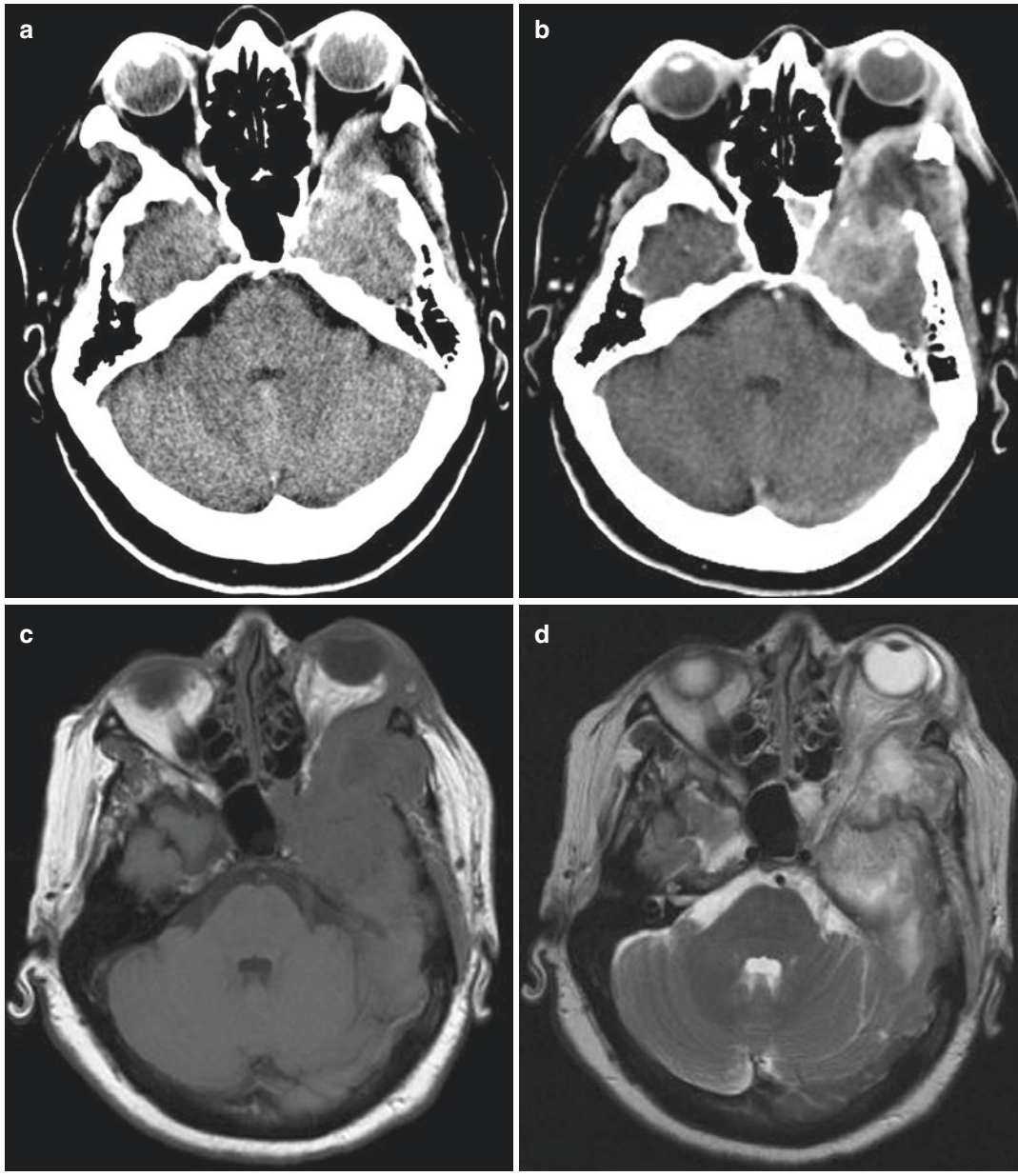

Fig. 13.6 (**a**) Axial non-contrast CT demonstrates a left temporal lobe mass destroying the greater wing of the sphenoid bone and invading into the orbit and the infratemporal fossa. (**b**) Axial contrast-enhanced CT better demonstrates the mass with heterogeneous enhancement. (**c**) Axial T1-weighted MRI demonstrated a heterogeneous hypointense mass involving the anterior left temporal lobe with left sphenoid bone destruction. (**d**) Axial T2-weighted MRI demonstrates the tumour to be heterogeneous isointense to brain cortex with central hyperintense areas of necrosis. (**e**) Contrast-enhanced axial T1-weighted MRI demonstrates heterogeneous enhancement with central necrosis intracranially. (**f**) Sagittal contrast-enhanced T1-weighted demonstrates heterogeneous enhancement in the anterior more solid part of the tumour and a posterior cystic component with an irregular rim of enhancement

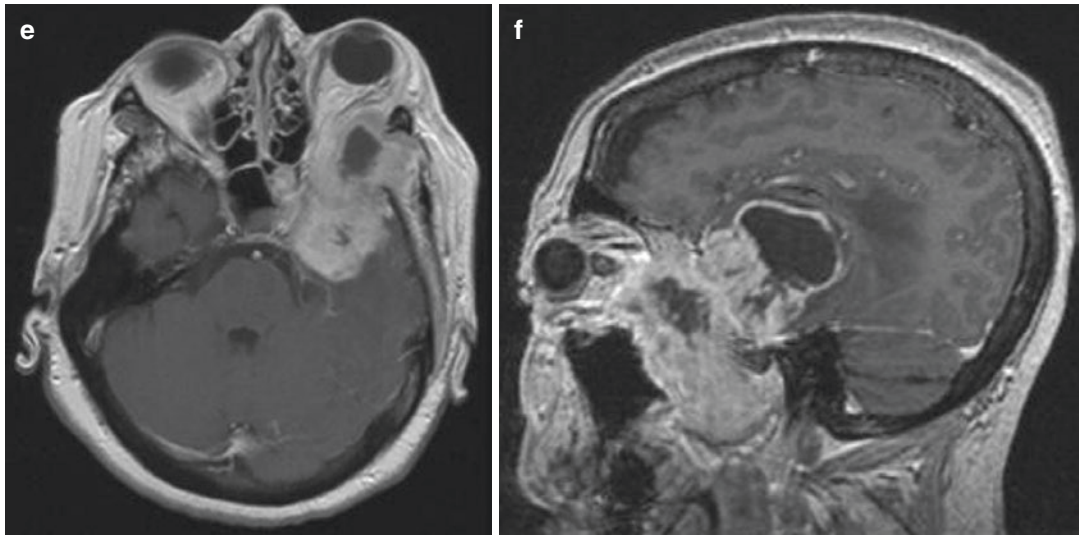

Fig. 13.6 (continued)

13.6.2 Epidemiology

Gliosarcomas represent 2% of the malignant primary glial tumours; they occur in the fifth to sixth decade of life, they are more frequently located in the temporal lobe.

Eleven percent of the cases present with haematogenous metastases, the most frequent sites are lung 72%, liver 41%, and lymph nodes 18%.

Skull base invasion is a rare feature, the mechanism o extradural and extracranial extension is not well understood, but it is thought to be by dural invasion.

13.6.3 Pathology and Genetics

Gliosarcoma is a rare central nervous system (CNS) tumour, characterised by a biphasic tissue pattern, with alternating areas of glial origin with mixed areas of malignant mesenchymal differentiation. The main prognostic factor is the predominance of the sarcomatous component with better prognosis in those cases.

13.6.4 Clinical Management

Gliosarcomas have similar clinical and radiological presentation as glioblastoma (GB) and an even poorer prognosis.

Chemotherapy and radiotherapy is the treatment of choice although there is a debate over the value of TMZ chemotherapy.

13.6.5 Imaging Findings and Differential Diagnosis

Gliosarcomas tend to show variable characteristics on Magnetic Resonance Images. They are generally hypointense on T1-weighted images and hyperintense on T2-weighted images in comparison to white matter, with marked peritumoural oedema. On contrast images they present heterogeneous enhancement, with intense peripheral or irregular ring and central necrosis or cystic changes. Perfusion images show increased rCBV in solid enhancing areas. On diffusion images the solid areas can depict decreased ADC values. MR

spectroscopy shows increased Cho and Lac values and decreased NAA and Cr values.

Differential diagnosis includes glioblastomas, meningiomas, embryonal tumours and brain abscesses.

Take-Home Messages

- Gliosarcomas are superficially located tumours with a dural base. The most common site is the temporal lobe

Further Reading

1. Sampaio L, Linhares P, Fonseca J. Detailed magnetic resonance imaging features of a case series of primary gliosarcoma. Neuroradiol J. 2017; 30:546–553
2. Yi X, Cao H, Tang H, Gong G, Hu Z, Liao W, Sun L, Chen BT, Li X. Gliosarcoma: a clinical and radiological analysis of 48 cases. Eur Radiol. 2019; 29:429–438
3. Kozak KR, Mahadevan A, Moody JS. Adult gliosarcoma: epidemiology, natural history, and factors associated with outcome. Neuro Oncol. 2009; 11:183–91
4. Zhang BY, Chen H, Geng DY, Yin B, Li YX, Zhong P, Wu JS, Wang XQ. Computed tomography and magnetic resonance features of gliosarcoma: a study of 54 cases. J Comput Assist Tomogr. 2011; 35:667–73
5. Han L, Zhang X, Qiu S, Li X, Xiong W, Zhang Y, Qu H, Chang R, Chen B, Wang W, Li S. Magnetic resonance imaging of primary cerebral gliosarcoma: a report of 15 cases. Acta Radiol. 2008; 49:1058–67

13.7 Case 7

40-year-old female with a 3-month history of gait disturbance, bilateral facial hypoesthesia and visual deficit.

The patient deteriorated rapidly, therefore surgical biopsy of the tumour was not feasible; no histopathological confirmation was possible.

Based on the imaging appearance, large infiltrating tumour, with areas of enhancement and necrosis, the diagnosis of diffuse midline glioma was made and the patient underwent treatment with radiotherapy and concomitant temozolomide.

13.7.1 Images and Legends

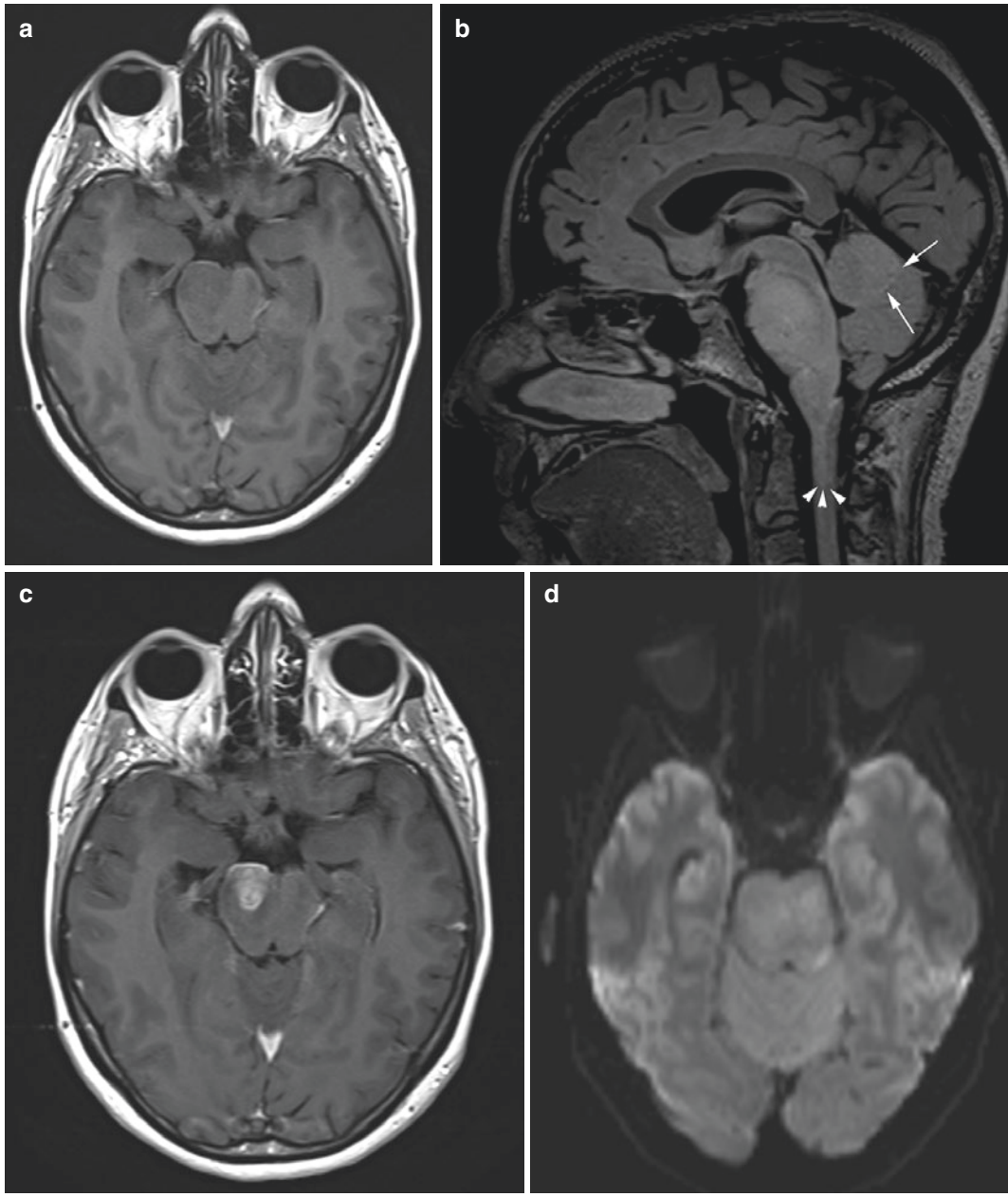

Fig. 13.7 (**a**) Axial T1-weighted MRI demonstrates a hypointense pontine mass with poorly defined margins. (**b**) Sagittal FLAIR MRI hyperintense shows the infiltrative expansile lesion involving the entire pons, vermis white arrows), caudal extension to the medulla (white arrowheads). (**c**) Contrast-enhanced axial T1-weighted image demonstrates a ringlike pattern of enhancement, suggesting central necrosis, on the right aspect of the pons, abutting the basilar artery. (**d**) Axial diffusion-weighted magnetic resonance imaging (DWI) the tumour demonstrates low signal on diffusion. (**e**) Apparent diffusion coefficient map (ADC). High ADC value is demonstrated within the tumour. (**f**) Dynamic susceptibility contrast-enhanced MR image. Relative cerebral blood volume (rCBV) colour map. Increased blood volume within the tumour. (**g**) ^{1}H-MR spectroscopy (TE 30 ms) shows an elevated choline (Ch) peak, reduced peak of N-acetyl aspartate (NAA) and elevated lipids and lactic acid peaks (lip-lac)

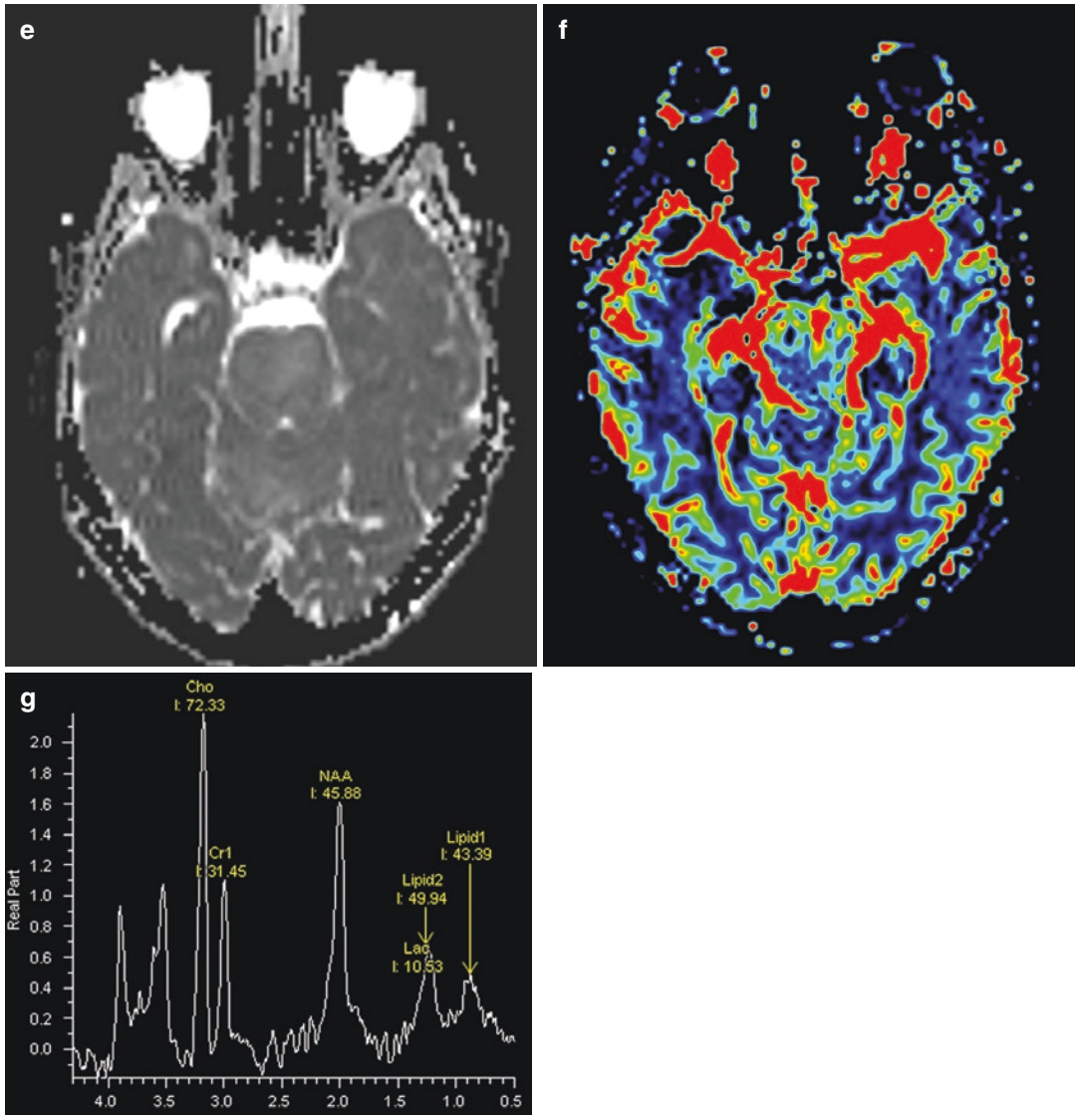

Fig. 13.7 (continued)

13.7.2 Epidemiology

Although brainstem tumours are more commonly encountered in children and represent 10% of all paediatric brain tumours, they represent only 1–2% of all brain tumours in adults.

Brainstem tumours are more frequently found in children, adult brainstem tumours represent 1–2% of all brain tumours in adults.

13.7.3 Pathology and Genetics

Based on the imaging features brain stem gliomas can be classified in four subgroups: diffuse intrinsic, low-grade brainstem gliomas involving>50% of the greatest dimension of the brainstem; focal, malignant brainstem gliomas; focal, tectal gliomas; and exophytically growing tumours.

In the revised 2016 World Health Organization classification, "Diffuse midline glioma, H3 K27M-mutant" is recognised as a distinct entity that corresponds to grade IV.

13.7.4 Clinical Management

These tumours occur in young adults in their third to fifth decade of life. The symptoms are insidious including gait disturbance, facial palsy, myasthenia, and cranial nerve deficits.

Radiotherapy is the standard treatment for adult brainstem gliomas, adjuvant chemotherapy is also used, although the role of chemotherapy remains unclear.

13.7.5 Imaging Findings and Differential Diagnosis

Diffusely infiltrating brainstem gliomas are characterised on MRI as ill-defined mass lesions T1-hypointense and T2-hyperintense with variable contrast enhancement. The presence of contrast enhancement within the tumour often is an indication of a higher pathologic grade and a worse prognosis.

Differential diagnosis includes demyelinating diseases, neuro-Behçet, lymphoma and sarcoidosis.

Take-Home Messages

- Diffuse midline gliomas present as infiltrating masses with expansion of the brainstem
- They depict increased signal on T2-weighted MRI sequences
- Frequently present contrast-enhancing areas with central necrosis

Further Reading

1. Aboian MS, Solomon DA, Felton E, Mabray MC, Villanueva-Meyer JE, Mueller S, Cha S. Imaging characteristics of pediatric diffuse midline gliomas with histone H3 K27 M mutation. AJNR 2017; 38:795–800
2. Louis DN, Perry A, Reifenberger G, von Deimling A, Figarella-Branger D, Cavenee WK, Ohgaki H, Wiestler OD, Kleihues P, Ellison DW. The 2016 World Health Organization Classification of Tumors of the Central Nervous System: a summary. Acta Neuropathol. 2016; 131:803–20
3. Eisele SC, Reardon DA. Adult Brainstem Gliomas. Cancer 2016; 122:2799–809
4. Donaldson SS, Laningham F, Graham Fisher PG. Advances Toward an Understanding of Brainstem Gliomas. J Clin Oncol 2006; 1266–1272
5. Purohit B, Kamli AA, Kollias SS. Imaging of adult brainstem gliomas. Eur J Radiol. 2015; 84:709–20

13.8 Case 8

45-year-old female presenting to the emergency room with generalised tonic-clonic seizure after a gustatory aura. The patient presented prior episodes of gustatory and olfactory sensations. She refers a yearlong period of fluctuating headache.

Patient underwent near complete total resection of the right frontal part of the tumour, no further treatment was implemented. She continues under close surveillance.

Histology revealed an oligodendroglioma WHO grade II. Molecular and genetic features: Isocitrate dehydrogenase (IDH1)-mutant, 1p/19q codeleted and P53 negative.

13.8.1 Images and Legends

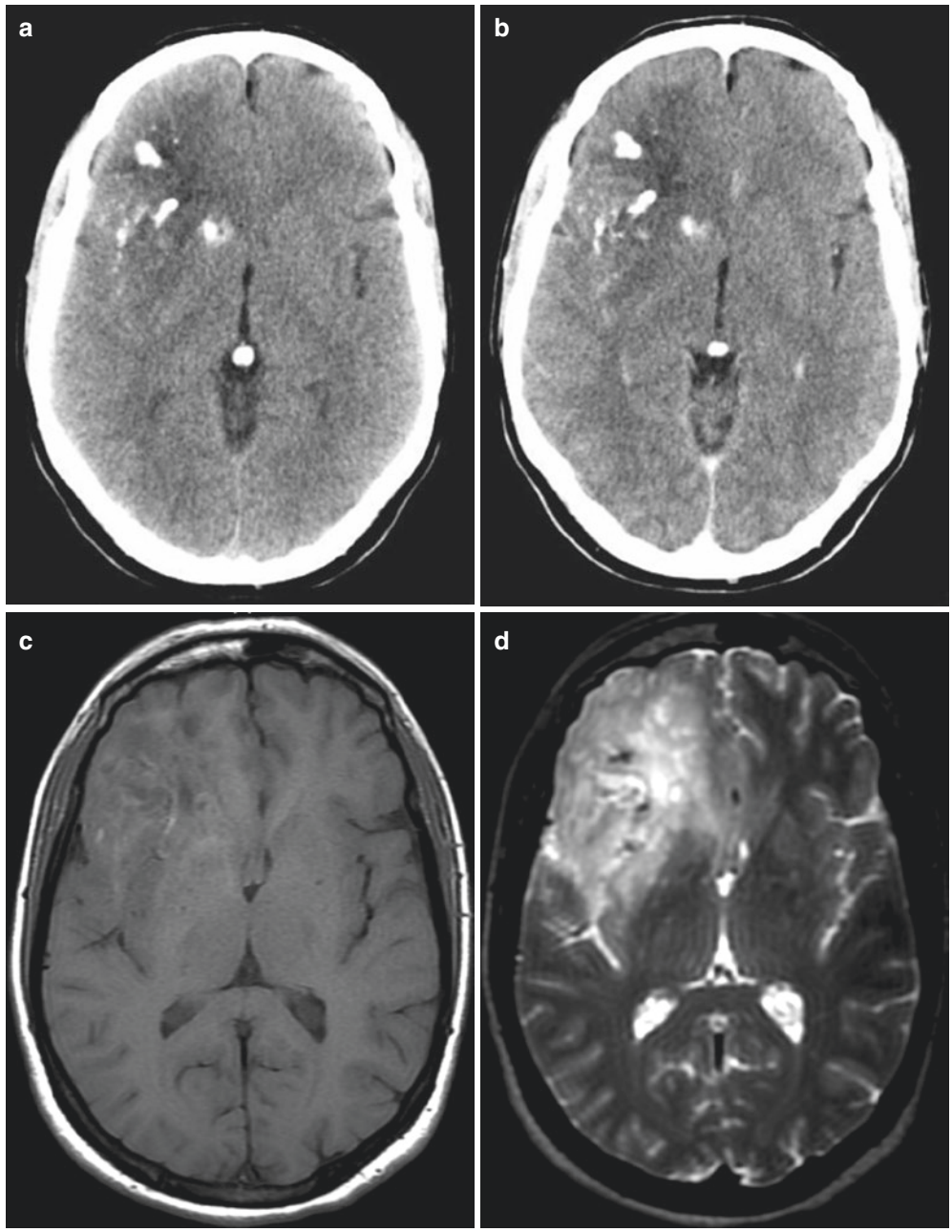

Fig. 13.8 (**a**) Axial non-enhanced brain CT demonstrates a large ill-defined, hypoattenuating frontal mass with coarse calcifications. (**b**) Axial contrast-enhanced CT demonstrating the same features with no areas of enhancement within the tumour. (**c**) Axial T1-weighted MRI shows a large right frontal mass with poorly defined borders and internal heterogeneity with some linear high signal intensity areas. (**d**) Axial T2-weighted MRI shows the mass predominantly hyperintense with internal heterogeneity and mass effect abutting the frontal horn of the right ventricle. (**e**) Axial FLAIR MRI better demonstrates the wide involvement in the cortex and subcortical white matter in the frontal and insular lobes extending through the genu of the corpus callosum into the left frontal lobe. (**f**) Contrast-enhanced axial T1-weighted image shows scattered areas of faint enhancement within the tumour. (**g**) Axial diffusion-weighted magnetic resonance imaging (DWI) shows low signal intensity of the mass. (**h**) Apparent diffusion coefficient map (ADC). The tumour shows high ADC value, indicating absence of restricted water diffusion. (**i**) Dynamic susceptibility contrast-enhanced MR image. Relative cerebral blood volume (rCBV) colour map. The tumour shows mildly increased rCBV. (**j**) ^{1}H-MR spectroscopy (TE 135 ms) shows a slightly elevated choline (Ch) peak and reduced peak of N-acetyl aspartate (NAA)

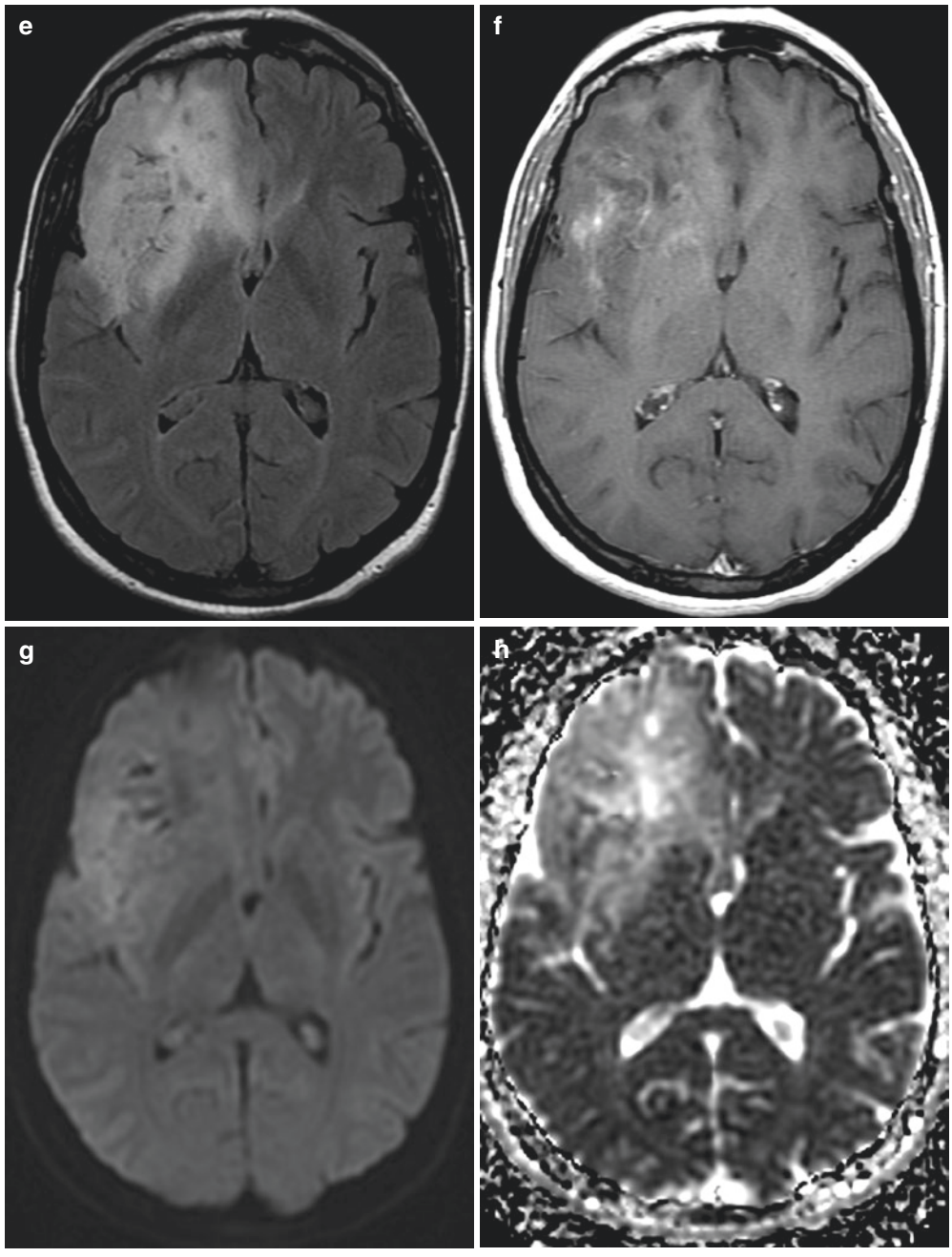

Fig. 13.8 (continued)

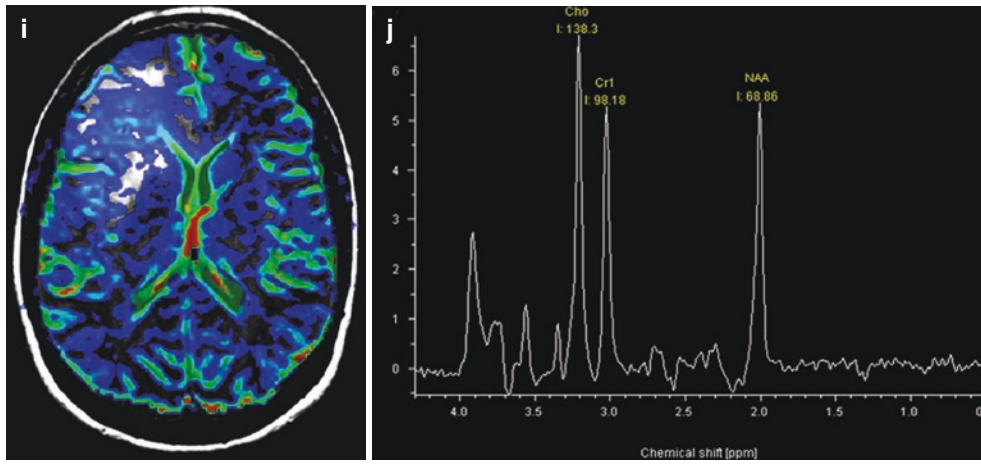

Fig. 13.8 (continued)

13.8.2 Epidemiology

Oligodendroglioma is the third most common glioma it accounts for 5–20% of all glial tumours. They occur predominantly in adults; with a peak between 40 and 60 years, males are more commonly affected. Seizure activity is the most common clinical presentation.

13.8.3 Pathology and Genetics

Oligodendrogliomas are defined as IDH-mutant and 1p/19q-codeleted grade II tumours by the 2016 WHO classification.

13.8.4 Clinical Management

Surgical resection and gross total resection is the principal form of therapy in oligodendrogliomas.

13.8.5 Imaging Findings and Differential Diagnosis

Frontal lobe location (50% of the cases), cortical involvement and calcification are common among low-grade oligodendrogliomas, mucoid or cystic degeneration are also frequently found. The temporal lobe is the second most common location.

On imaging oligodendrogliomas usually are hypointense compared to grey matter on T1-weighted images and hyperintense compared to grey matter on T2-weighted images, with heterogeneous signal intensity within the tumour. Vasogenic oedema surrounding the tumour is not commonly seen. Low-grade oligodendrogliomas usually do not enhance after contrast administration, some cases may depict minimal, multifocal enhancement with a dot-like or lacy pattern.

Oligodendrogliomas may have markedly elevated rCBV even when low-grade, elevated rCBV does therefore not necessarily indicate high-grade tumour in oligodendroglioma.

Low-grade oligodendroglioma shows moderately elevated Cho and decreased NAA without a lactate peak.

Take-Home Messages

- Cortical grey matter involvement, frontal lobe location and calcifications are highly distinctive features in oligodendrogliomas
- Oligodendroglioma might have markedly elevated rCBV even low grade ones; this finding is attributed to the presence of the short capillary segments in oligodendroglioma

Further Reading

1. Lin Y, Xing Z, She D, Yang X, Zheng Y, Zebin Xiao Z, Wang X, Dairong Cao D. IDH mutant and 1p/19q co-deleted oligodendrogliomas: tumor grade stratification using diffusion-, susceptibility-, and perfusion-weighted MRI. Neuroradiology 2017; 59:555–562
2. Fellah S, Caudal D, De Paula AM, Dory-Lautrec P, Figarella-Branger D, Chinot O, Metellus P, Cozzone PJ, Confort-Gouny S, Ghattas B, Callot V, Girard N. Multimodal MR Imaging (Diffusion, Perfusion, and Spectroscopy): Is it possible to distinguish oligodendroglial tumor grade and 1p/19q codeletion in the pretherapeutic diagnosis?. AJNR 2013; 34:1326–33
3. Johnson DR, Diehn FE, Giannini C, Jenkins RB, Jenkins SM, Parney IF, Kaufmann TJ. Genetically Defined Oligodendroglioma Is Characterized by Indistinct Tumor Borders at MRI. AJNR 2017; 38:678–684
4. Smits M. Imaging of oligodendroglioma. Br J Radiol 2016; 89: 20150857
5. Koeller KK, Rushing EJ. From the archives of the AFIP: Oligodendroglioma and its variants: radiologic-pathologic correlation. Radiographics. 2005; 25:1669–88

13.9 Case 9

45-year-old female with seizures.

Biopsy was performed; the pathological diagnosis was oligodendroglioma, Ki67 15%, WHO grade II. Molecular and genetic features: Isocitrate dehydrogenase (IDH1)-wild-type, ATRX positive (Wild-type), P53 negative. 1p19q codeletion positive. TERT mutation (c.-124 C > T).

13.9.1 Images and Legends

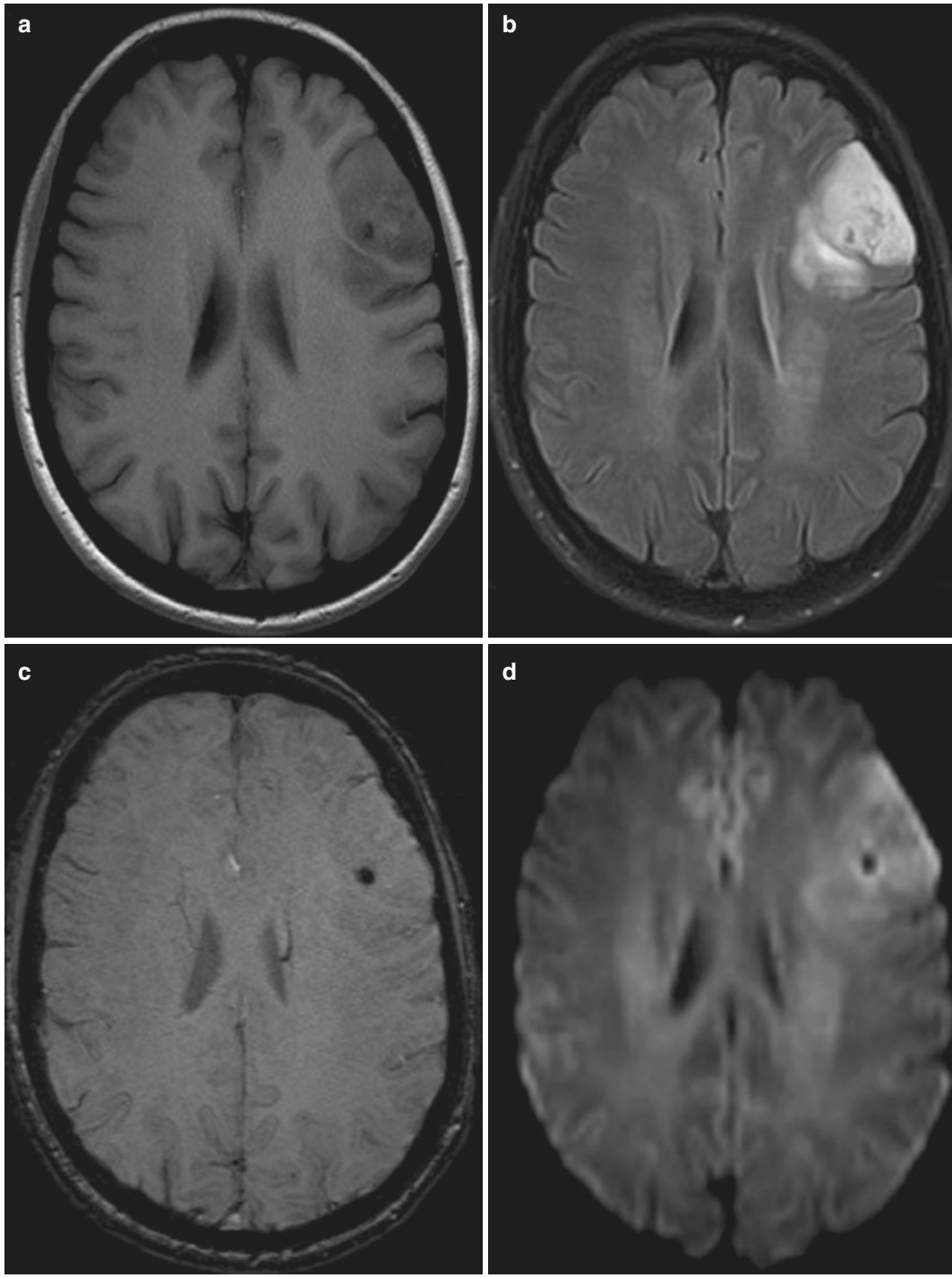

Fig. 13.9 (**a**) Axial T1-weighted MRI demonstrates an iso-hypointense solid mass involving the middle frontal gyrus. (**b**) Axial FLAIR MRI shows hyperintense heterogeneous solid mass with central hypointense areas surrounded by mild vasogenic oedema. (**c**) Axial SWI demonstrates susceptibility artefact inside the lesion from calcifications. (**d**) DTI demonstrates high signal in solid parts related to hypercellularity. (**e**) Low ADC values in solid enhancing areas. (**f**) MR perfusion shows rCBV elevated in solid enhancing regions of the tumour. (**g**) Contrast-enhanced axial T1-weighted MRI demonstrates heterogeneous mild enhancement. (**h**) MR spectroscopy shows increased Cho and decreased Cr and NAA

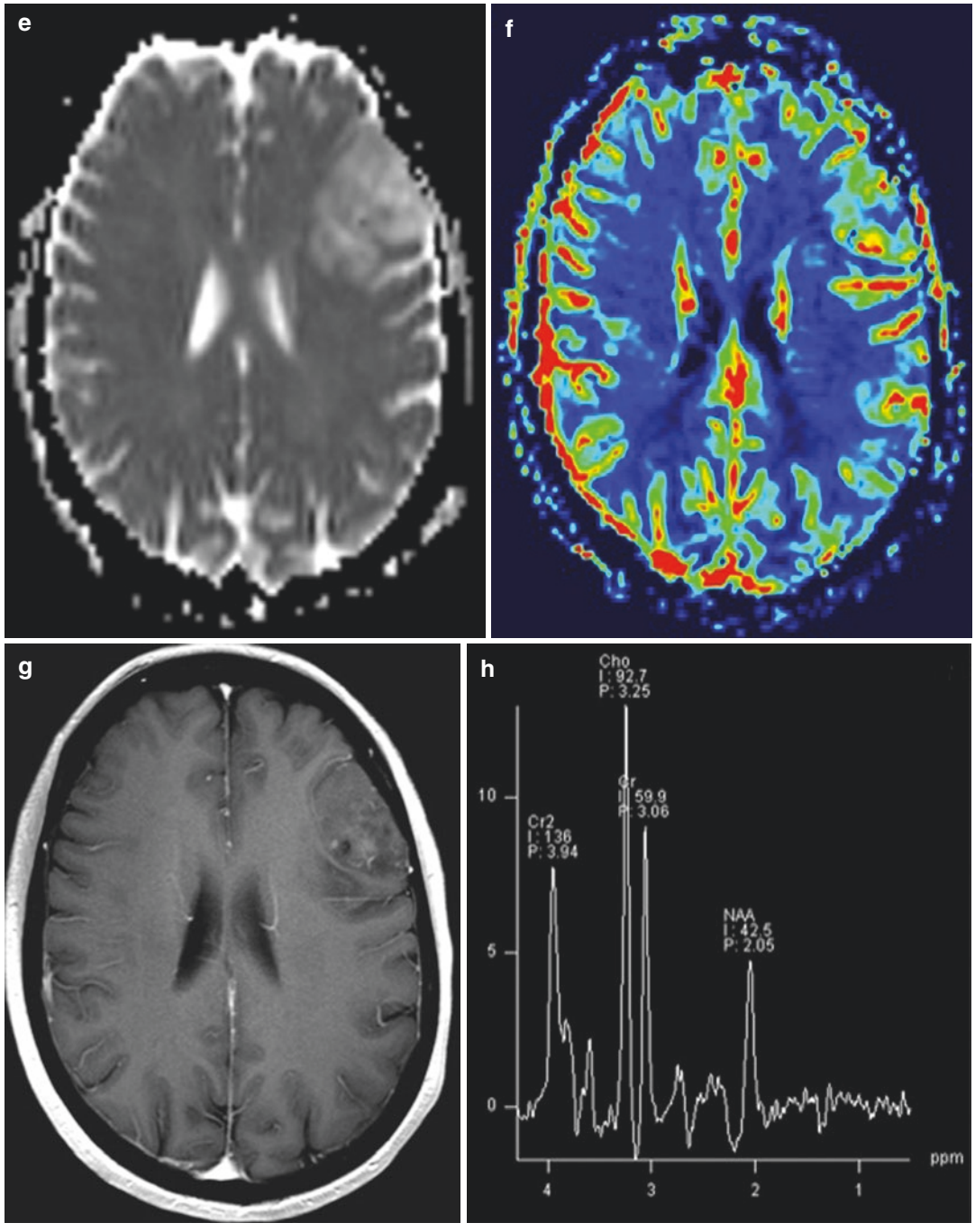

Fig. 13.9 (continued)

13.9.2 Epidemiology

Oligodendrogliomas are glial tumours more frequent in the fourth to fifth decade of life with slight male predilection. They account for 5–25% of all gliomas and 5–10% of all primary intracranial neoplasms.

13.9.3 Pathology and Genetics

The molecular hallmark of oligodendroglioma is codeletion 1p19q which is present in 60–90% of histopathologically diagnosed oligodendroglioma and have both diagnostic and prognostic value.

13.9.4 Clinical Management

The patient received surgical resection followed by radiotherapy plus chemotherapy (procarbazine + lomustine + vincristine).

The presence of 1p19q codeletion has prognostic and predictive relevance. Early chemotherapy + radiation therapy increases survival in patients with anaplastic oligodendroglioma compared with radiotherapy alone.

13.9.5 Imaging Findings and Differential Diagnosis

Oligodendrogliomas are usually well-circumscribed supratentorial cortical-based mass most commonly located in frontal lobes. They frequently appear hypointense in T1WI and hyperintense in T2/FLAIR with areas of signal loss/susceptibility artefact on SWI from calcifications and variable contrast enhancement.

Increased rCBV on perfusion-weighted imaging may be found in some low-grade oligodendrogliomas.

Signal heterogeneity, high rCBV and irregular borders of tumours are suggestive of the 1p/19q codeletion.

Differential diagnosis includes astrocytoma, ganglioglioma, dysembryoplastic neuroepithelial tumour (DNET) and pleomorphic xanthoastrocytoma.

Take-Home Messages

- Oligodendrogliomas are usually well-circumscribed supratentorial cortical-based mass most commonly located in the frontal lobes
- 1p/19q codeletion and IDH mutation are characterised by better prognosis and better response to chemotherapy

Further Reading

1. Fellah S, Caudal D, De Paula AM, Dory-Lautrec P, Figarella-Branger D, Chinot O, Metellus P, Cozzone PJ, Confort-Gouny S, Ghattas B, Callot V, Girard N. Multimodal MR imaging (diffusion, perfusion, and spectroscopy): is it possible to distinguish oligodendroglial tumor grade and 1p/19q codeletion in the pretherapeutic diagnosis? AJNR 2013; 34:1326–1333
2. Dumrongpisutikul N, Intrapiromkul J, Bonekamp D, Barker PB. Imaging Characteristics of Oligodendrogliomas. AJNR 2012; 33:1–6
3. Bourdillon P, Hlaihel C, Guyotat J, Guillotton L, Honnorat J, Ducray F, Cotton F. Prediction of anaplastic transformation in low-grade oligodendrogliomas based on magnetic resonance spectroscopy and 1p/19q codeletion status. J Neurooncol. 2015; 122:529–37
4. Spampinato MV, Smith JK, Kwock L, Ewend M, Grimme JD, Camacho DLA, et al. Cerebral blood volume measurements and proton MR spectroscopy in grading of oligodendroglial tumors. AJR 2007; 188:204–2012
5. Jenkinson MD, du Plessis DG, Smith TS, Joyce KA, Warnke PC, Walker C. Histological growth patterns and genotype in oligodendroglial tumours: correlation with MRI features. Brain. 2006; 129:1884–1891

13.10 Case 10

37-year-old man with headache, started several months ago.

Biopsy was performed; the pathological diagnosis was pilocytic astrocytoma, WHO grade I.

13.10.1 Images and Legends

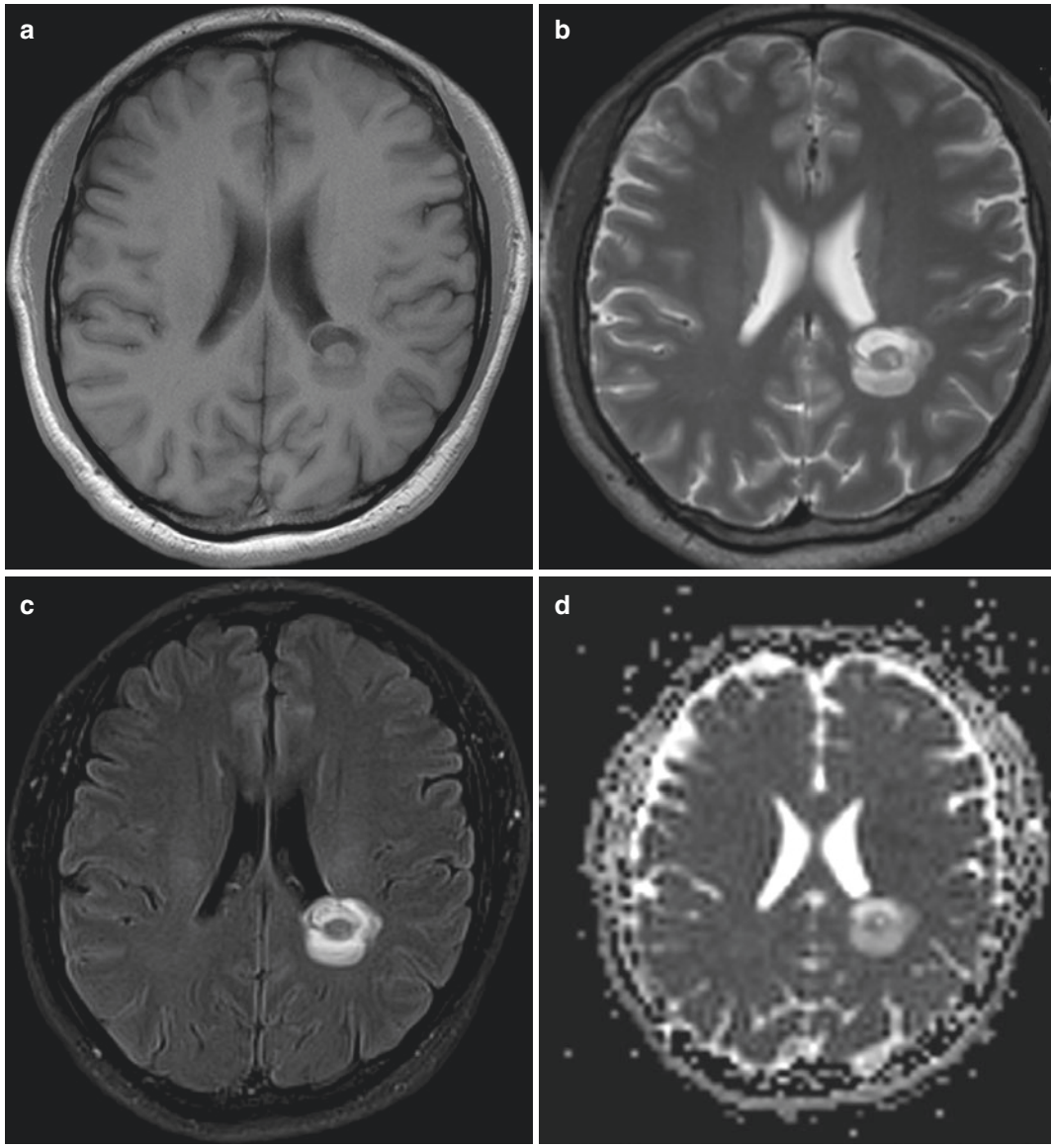

Fig. 13.10 (**a**) Axial T1-weighted MRI demonstrates a well-defined cystic mass with a hypointense peripheral nodule, adjacent to the occipital horn of the left lateral ventricle. (**b**) Axial T2WI demonstrates the solid and cystic components of the mass. No vasogenic oedema is seen. (**c**) FLAIR MRI shows the hyperintense solid nodule and the fluid signal cystic component. (**d**) Axial ADC map shows high signal with exception of the central nodule. (**e**) Axial SWI demonstrates small foci of signal loss that may be due to calcifications or haemorrhage. (**f**) Contrast-enhanced axial T1-weighted MRI demonstrates vivid enhancement in central nodule

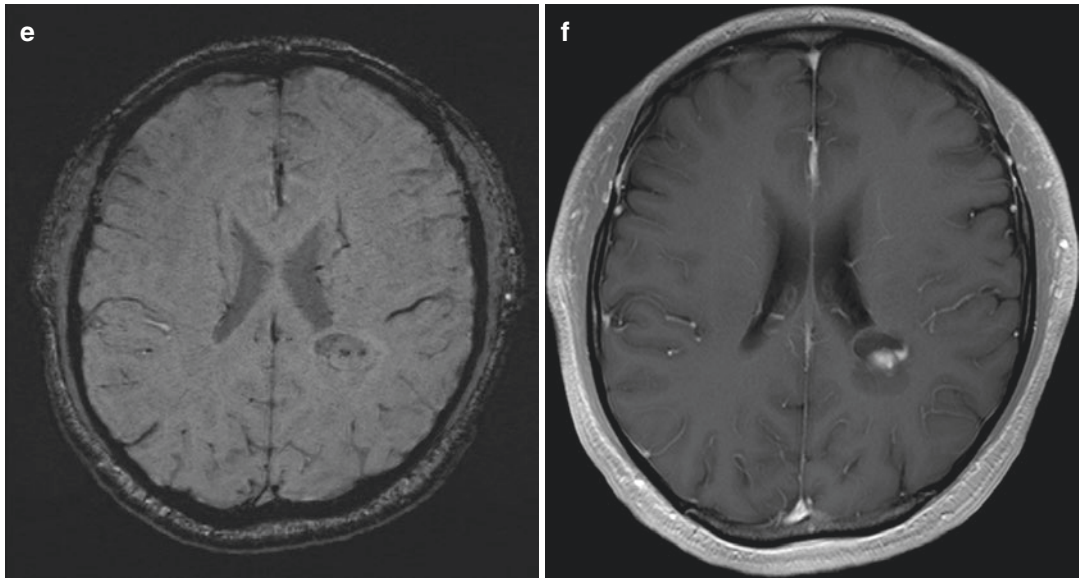

Fig. 13.10 (continued)

13.10.2 Epidemiology

Pilocytic astrocytomas tend to occur in young adults (first two decades of life), typically at 9–10 years.

They are the most common primary brain tumour of childhood and the most common paediatric cerebellar tumour (70–85% of all cerebellar astrocytomas).

13.10.3 Pathology and Genetics

The most common location is the cerebellum followed by the optic pathway, particularly in patients with NF1.

They frequently have BRAF alterations (about 70% of cases) and lack IDH and TP53 mutations.

13.10.4 Clinical Management

After a complete surgical resection, the patient remains disease-free until now.

13.10.5 Imaging Findings and Differential Diagnosis

Mixed masses with hypointense in T1WI and hyperintense in T2WI solid component, which shows strong enhancement, and fluid signal cystic component. ADC map shows typically high signal.

Differential diagnosis includes pleomorphic xanthoastrocytoma, medulloblastoma, ependymoma, haemangioblastoma, cerebellar abscess and ganglioglioma.

Take-Home Messages

- PA are the most common intracranial tumours in childhood and the most common paediatric cerebellar tumour
- There are mixed masses with solid component that shows vivid enhancement and cystic component

Further Reading

1. Chourmouzi D, Papadopoulou E, Konstantinidis M, Syrris V, Kouskouras K, Haritanti A, et al. Manifestations of pilocytic astrocytoma: A pictorial review. Insights Imaging. 2014; 5:387–402
2. Murakami R, Hirai T, Kitajima M, Fukuoka H, Toya R, Nakamura H, et al. Magnetic resonance imaging of pilocytic astrocytomas: Usefulness of the minimum Apparent Diffusion Coefficient (ADC) value for differentiation from high-grade gliomas. Acta radiol. 2008; 49:462–7
3. Koeller KK, Rushing EJ. From the Archives of the AFIP. RadioGraphics 2004; 24:1693–1708

13.11 Case 11

46-year-old female with a previous history of chronic headaches and depression. The patient present left face myoclonus and focal epilepsy with posterior generalisation. Surgery was performed. The specimen showed an oligodendroglial cell population with cystic component and small gliosis in the periphery of the tumour. Ki67 lower than 1%, no IDH or p53 mutation is demonstrated. The sample was positive in GFAP immunochemistry stain. No mitosis, necrosis or perivascular proliferation is noted. Dysembryoplastic neuroepithelial tumour (DNET) was diagnosed.

13.11.1 Images and Legends

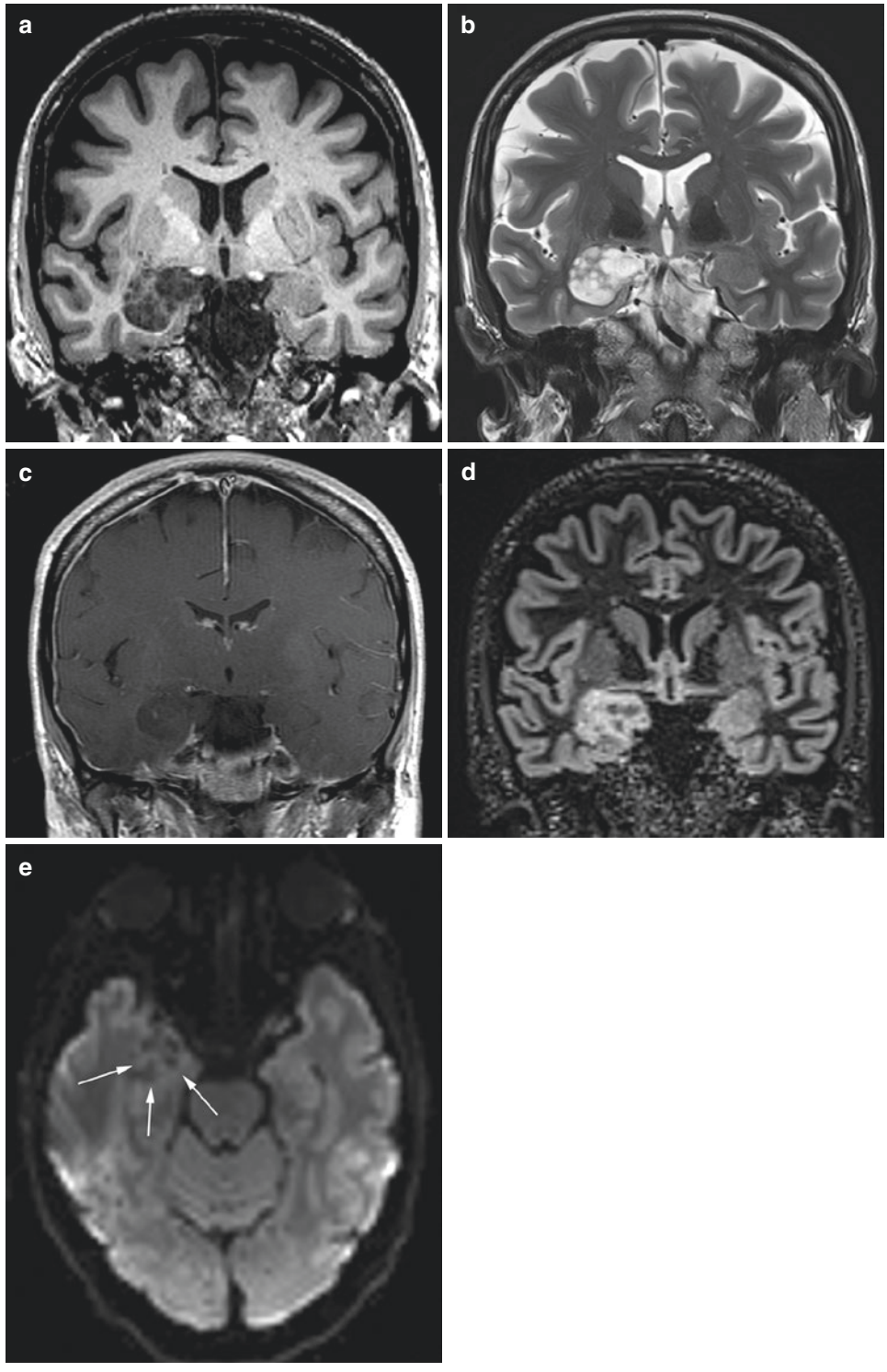

Fig. 13.11 (**a**) Coronal T1W MRI demonstrates a mass in the right hippocampus. (**b**) Coronal T2W MRI, the mass shows a multicystic "bubbly" appearance with cyst following the CSF signal and slight mass effect. (**c**) Coronal contrast-enhanced T1W MRI. No enhancement is noted in the lesion. (**d**) Coronal Double Inversion Recovery (DIR) MRI. High signal is noted in the lesion. There is a hyperintensity halo around the lesion. (**e**) Axial DWI MRI No restriction is demonstrated (arrows)

13.11.2 Epidemiology

DNET is juvenile or infantile tumour with a slight predilection in males.

13.11.3 Pathology and Genetics

DNET is a WHO I class tumour. It derivates from cortical grey matter and has a predilection for the temporal lobe. The characteristic pathologic feature is the Specific Glioneuronal Element (SGNE). There is association with focal cortical dysplasia. Intractable partial seizures are typical clinical debut.

DNETs are negative for IDH mutations, P53 mutations, and do not demonstrate 1p19q deletion. SGNE is positive for GFAP. Oligodendroglia inside the tumour shows S100 and OLIG2 positivity.

13.11.4 Clinical Management

DNET do not grow over time, however, seizures are usually intractable so surgery is warranted. Prognosis is excellent.

13.11.5 Imaging Findings and Differential Diagnosis

DNETs are cortical lesions with a "bubbly" appearance and cystic areas. Typically there is no enhancement. Susceptibility weighted images (SWI) or CT are very useful for demonstrating calcification of the lesion. No DWI restriction or rCBV hypervascularization is present. Temporal lobe is affected in over 50% of cases. Typical differentials are ganglioglioma, pleomorphic xanthoastrocytoma, oligodendroglioma and cystic lesions (neuroepithelial, choroid fissure).

Take-Home Messages

- Young patient with partial, persistent seizures and a temporal "bubbly" mass is typically a DNET

Further Reading

1. Takahashi A, Hong SC, Seo DW et al. Frequent association of cortical dysplasia in dysembryoplastic neuroepithelial tumor treated by epilepsy surgery. Surg Neurol. 2005; 64: 419–427
2. Makola M, Cecil KM. Dysembryoplastic neuroepithelial tumor (DNET) and focal cortical dysplasia: Case report of two pediatric patients with imaging features. International Journal of Diagnostic Imaging. 2017; 4:31
3. Isler C, Erturk Cetin O, Ugurlar D, Ozkara C, Comunoglu N, Kizilkilic O, Oz B, Kayadibi Y, Tanriverdi T, Uzan M. Dysembryoplastic neuroepithelial tumours: clinical, radiological, pathological features and outcome. British journal of neurosurgery. 2018; 23:1–6
4. Cosson RS, Varlet P, Beuvon F, Duport CD, Devaux B, Chassoux F, Fredy D, Meder JF. Dysembryoplastic neuroepithelial tumors: CT, MR findings and imaging follow-up: a study of 53 cases

13.12 Case 12

35-year-old male with a recent onset of seizures.

Biopsy was performed; the pathological diagnosis was Ganglioglioma, WHO grade I.

13.12.1 Images and Legends

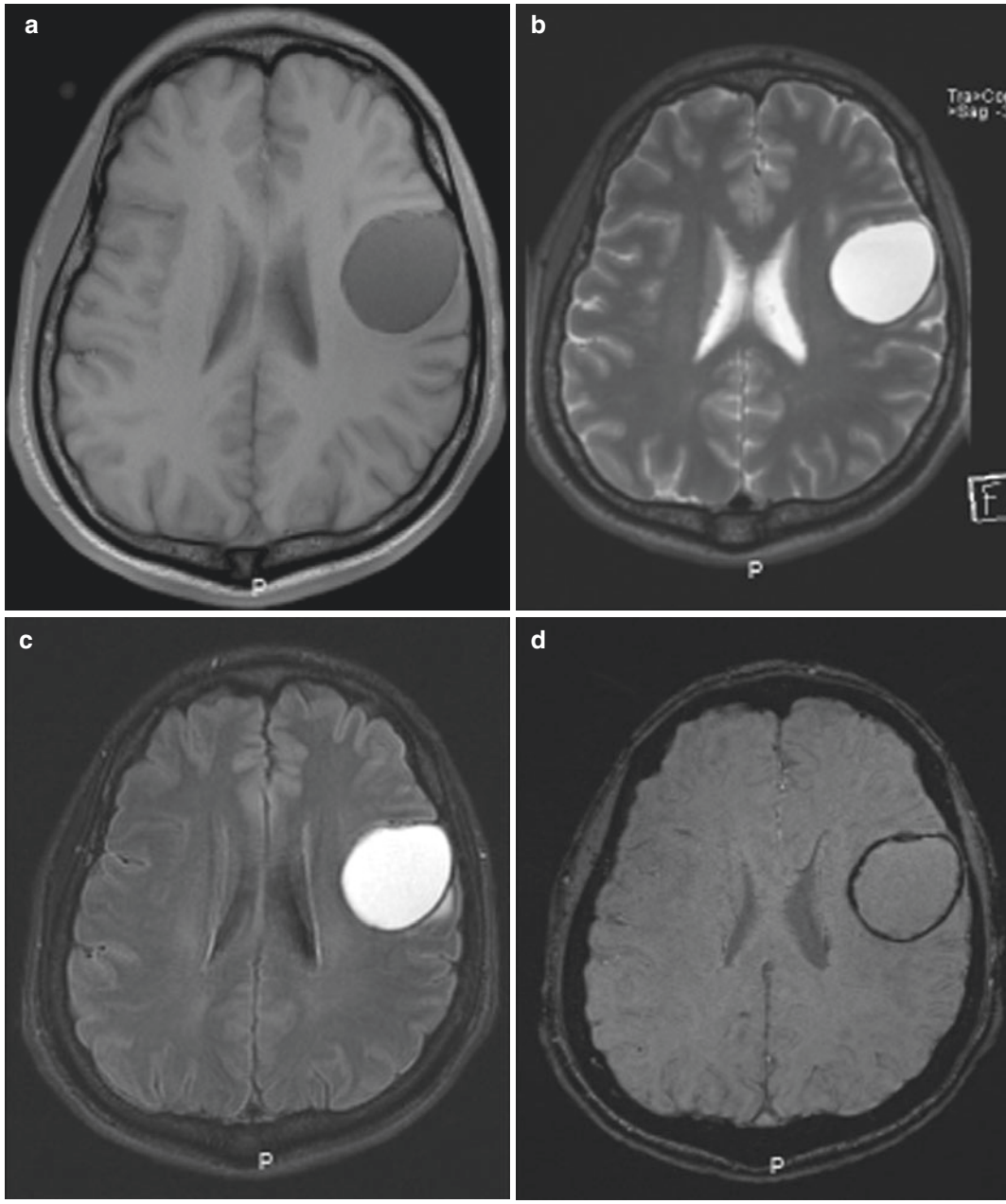

Fig. 13.12 (**a**) Axial T1-weighted MRI demonstrates a cortical-based hypointense mass in left frontal lobe surrounded by a hypointense thin rim. (**b**) Axial T2WI shows a fluid signal cystic mass in left frontal lobe. (**c**) Axial FLAIR MRI shows hyperintense content of the cystic lesion that could be related with high protein content. There is no vasogenic oedema. (**d**) Axial SWI demonstrates thin hypointense peripheral rim may be due to calcification. (**e**) Axial ADC map shows high signal within the mass. (**f**) Contrast-enhanced axial T1-weighted MRI demonstrates mild peripheral enhancement, which predominates in anterior part of the lesion. (**g**) Axial Non-Contrast CT scan confirms thin calcification of peripheral rim

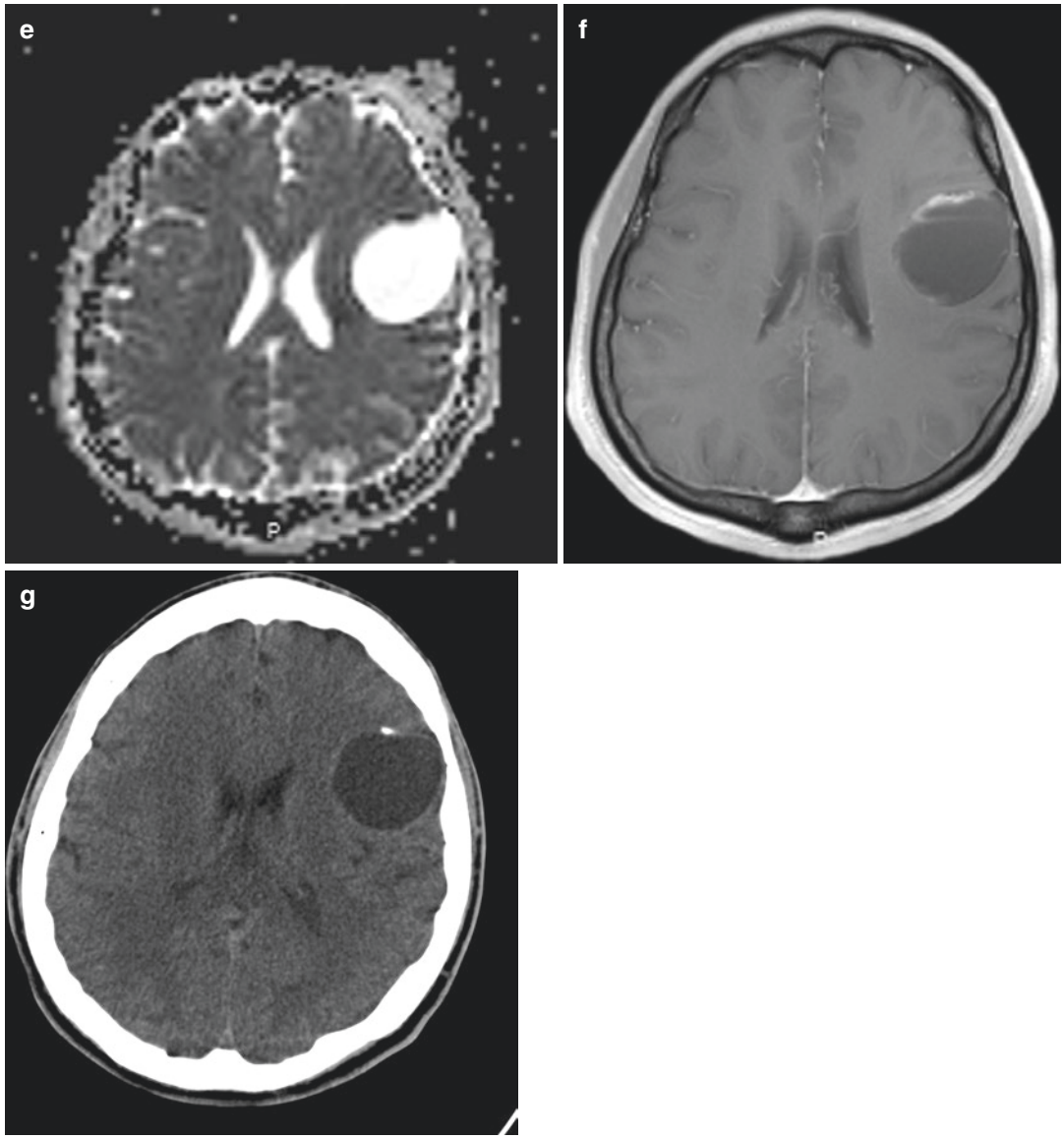

Fig. 13.12 (continued)

13.12.2 Epidemiology

These tumours represent 0.4–0.9% of all primary brain tumours in adults and about 10% of all primary brain tumours in children.

Most of gangliogliomas are found in infants or young individuals aged 8–31 years with no gender predominance.

13.12.3 Pathology and Genetics

The majority of them occur in temporal lobes and in the cerebellar hemispheres.

BRAF V600E mutations are found in 20–60% of cases. IDH negative.

13.12.4 Clinical Management

After a complete surgical resection, the patient remains disease-free until now.

13.12.5 Imaging Findings and Differential Diagnosis

Variable appearance on MRI. Predominantly cystic masses with variable signal in the cystic component in T2WI related to the amount of proteinaceous material or blood products. Iso to hypointense solid component in T1WI with variable contrast enhancement. Blooming signal loss in T2*/SWI due to calcified areas.

Differential diagnosis includes dysembryoplastic neuroepithelial tumours (DNET), pleomorphic xanthoastrocytoma, oligodendroglioma and desmoplastic infantile astrocytoma and ganglioglioma.

Take-Home Messages

- Tumours with peripheral location within cerebral hemispheres with predilection for temporal and frontal lobes and variable appearance on MRI

Further Reading

1. Castillo M. Gangliogliomas: Ubiquitous or not? Am J Neuroradiol. 1998; 19:807–809
2. Jong Won Kwon, Kim IO, Cheon JE, Woo Sun Kim, Je Geun Chi, Wang KC, et al. Cerebellopontine angle ganglioglioma: MR findings. Am J Neuroradiol. 2001; 22:1377–1379
3. Provenzale JM, Ali U, Barboriak DP, Kallmes DF, Delong DM, McLendon RE. Comparison of patient age with MR imaging features of gangliogliomas. AJR Am J Roentgenol. 2000; 174:859–862

13.13 Case 13

23-year-old male who consulted the emergency department for cervical pain, headache, confusion and general deterioration with walking difficulty.

Patient underwent surgery; the mass was attached to the tentorium and completely removed.

The pathological diagnosis was classic medulloblastoma with some areas of the desmoplastic variant, Ki67 30%, WHO grade IV. Molecular and genetic features: CD45, CD20, p53, CD99 and c-erbB2 negative.

The patient underwent radiotherapy after surgery.

13.13.1 Images and Legends

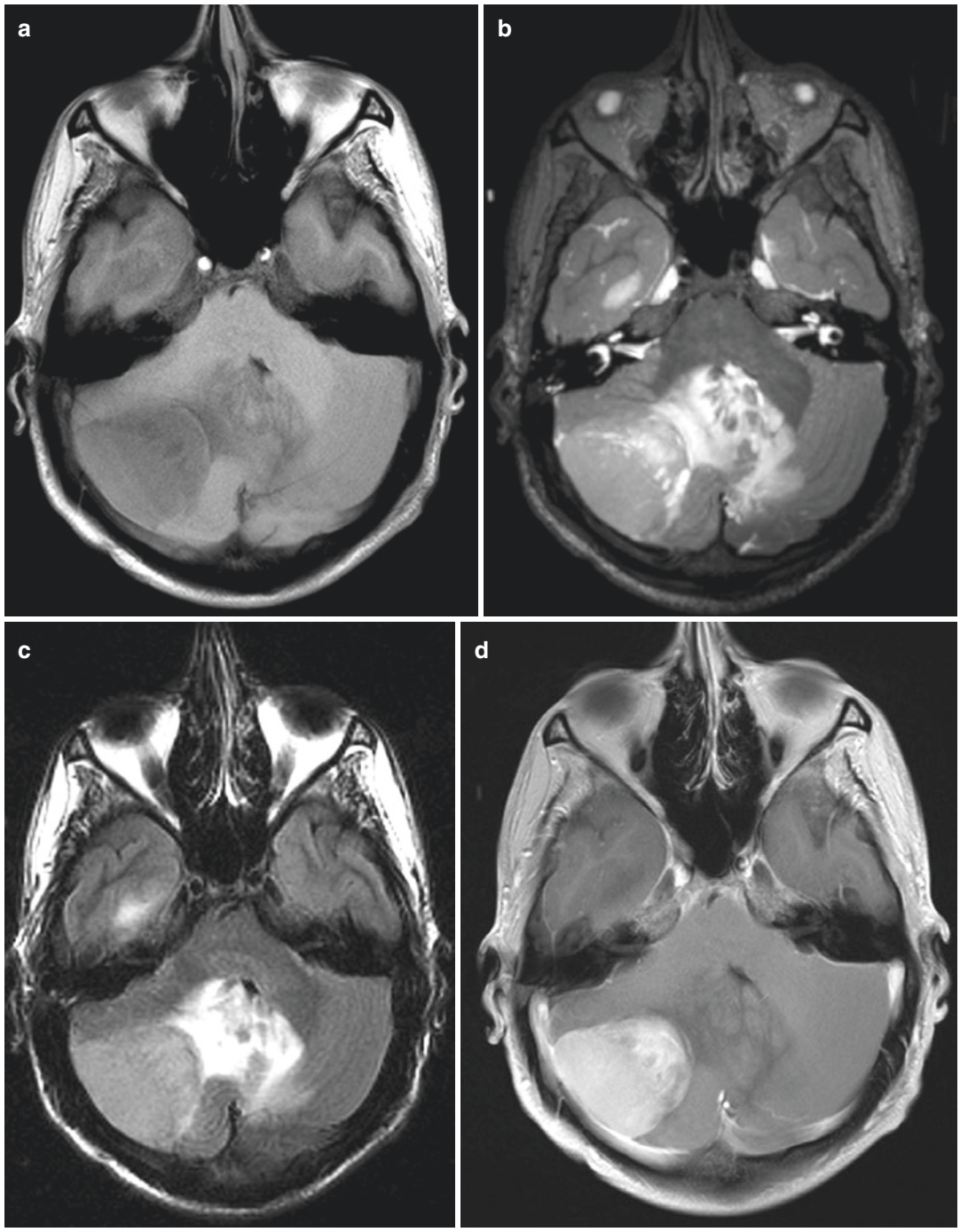

Fig. 13.13 (**a**) Axial T1-weighted MRI reveals a right cerebellar isointense, hemispheric mass. (**b**) Axial T2-weighted MRI. Heterogeneous mostly isointense mass with cysts and necrotic changes. (**c**) Axial FLAIR MRI demonstrating the mass, severe vasogenic oedema, midline shift and mass effect over the fourth ventricle. (**d**) Contrast-enhanced axial T1-weighted image shows a well-defined mass with heterogeneous enhancement. (**e**) Axial diffusion-weighted magnetic resonance imaging (DWI) shows increased diffusion signal due to water movement limitation. (**f**) Apparent diffusion coefficient map (ADC). The tumour demonstrates low ADC value, which reflects high cellular density. (**g**) Dynamic susceptibility contrast-enhanced MR image. Relative cerebral blood volume (rCBV) colour map. The tumour shows mainly a low rCBV, with some central areas with slightly increased rCBV. (**h**) ^{1}H-MR spectroscopy (TE 30 ms) shows an elevated choline (Ch) peak, reduced peak of N-acetyl aspartate (NAA) and elevated lipids and lactic acid peaks (lip-lac)

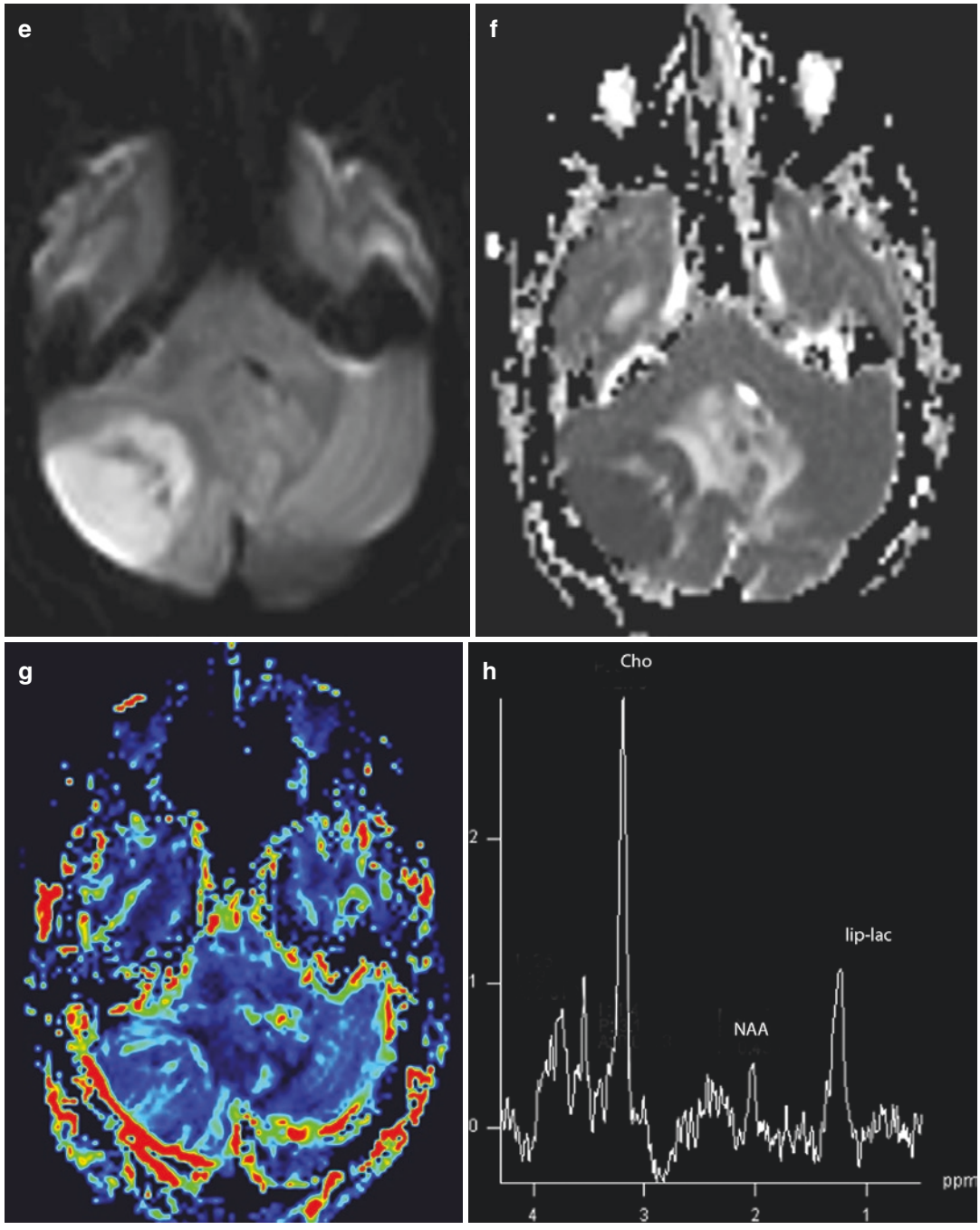

Fig. 13.13 (continued)

13.13.2 Epidemiology

Medulloblastoma is the most common cerebellar tumour in children <20 years. One-fourth occur in adulthood, mean age 31-years-old and more often are lateral hemispheric not midline vermian as in childhood.

13.13.3 Pathology and Genetics

The WHO regards all medulloblastomas as grade IV neoplasms. There are four major histologic subtypes: classic, desmoplastic/nodular, extensively nodular, and large cell/anaplastic. In the new 2016 CNS WHO classification there are four genetically defined subtypes of medulloblastoma based on the presence or absence of activation in the wingless integration (WNT) or sonic hedgehog (SHH) signalling pathways: WNT-activated, SHH-activated and TP53-mutant, SHH-activated and TP53 wild-type, Non-WNT/non-SHH (groups 3 and 4).

13.13.4 Clinical Management

The four distinct molecular subgroups of medulloblastoma are clinically important. The definition of genetic and histologic features of medulloblastoma is necessary to define the adequate personalised therapy.

13.13.5 Imaging Findings and Differential Diagnosis

On imaging studies, medulloblastoma commonly appears as a well-defined enhancing posterior fossa mass with surrounding oedema, cyst formation, haemorrhage and occasional areas of calcification can be seen. Leptomeningeal seeding is common as high as 33% of the cases.

Medulloblastomas exhibit variable perfusion and permeability characteristics, with some lesions showing elevated perfusion and permeability and others not. Desmoplastic cases do not show elevation of the blood volume, which could be due to their fibrous matrix.

On MR spectroscopy, medulloblastomas demonstrate increased Cho peak and decreased NAA. Significant elevated Taurine (Tau) concentration at 3.3 ppm is seen in the classic subtype of medulloblastoma.

Take-Home Messages

- Four genetically defined subtypes of medulloblastoma have been added in the new WHO 2016 classification
- Medulloblastoma in the adulthood is more commonly located in the cerebellar hemispheres
- Medulloblastoma exhibits a variable perfusion and permeability characteristics
- MR imaging of the spinal axis should be performed at the time of initial work up of the primary tumour to rule out leptomeningeal spread

Further Reading

1. Shih RY. Smirniotopoulos JG. Posterior fossa tumours in adult patients. Neuroimag Clin N Am 2016; 26:493–510
2. de Oliveira F, Landeiro JA, de Castro I. Adult hemispheric cerebellar medulloblastoma. Surg Neurol Int. 2018; 9:34–47
3. Keil VC, Warmuth-Metz M, Reh C, Enkirch SJ, Reinert C, Beier D, Jones DTW, Pietsch T, Schild HH, Hattingen E, Hau P. Imaging biomarkers for adult medulloblastomas: genetic entities may be identified by their MR imaging radiophenotype. Am J Neuroradiol. 2017; 38:1892–1898
4. Shih RY, Koeller KK. Embryonal Tumors of the Central Nervous System. RadioGraphics 2018; 38:525–541
5. Koeller KK, Rushing EJ. Medulloblastoma: a comprehensive review with radiologic-pathologic correlation. RadioGraphics 2003; 23:1613–1637

13.14 Case 14

41-year-old male with gait disturbance and ataxia. The patient has a history of pancreatic cystic tumours and suspicion of Von Hippel-Lindau disease. MRI was performed, and a cerebellar mass was found. Surgery was performed. Histology showed a highly vascular tumour with vacuolated cells and cystic areas. No mitosis was demonstrated. Cells show positivity for NSE and S-100. Final diagnosis was haemangioblastoma of the CNS (WHO I).

13.14.1 Images and Legends

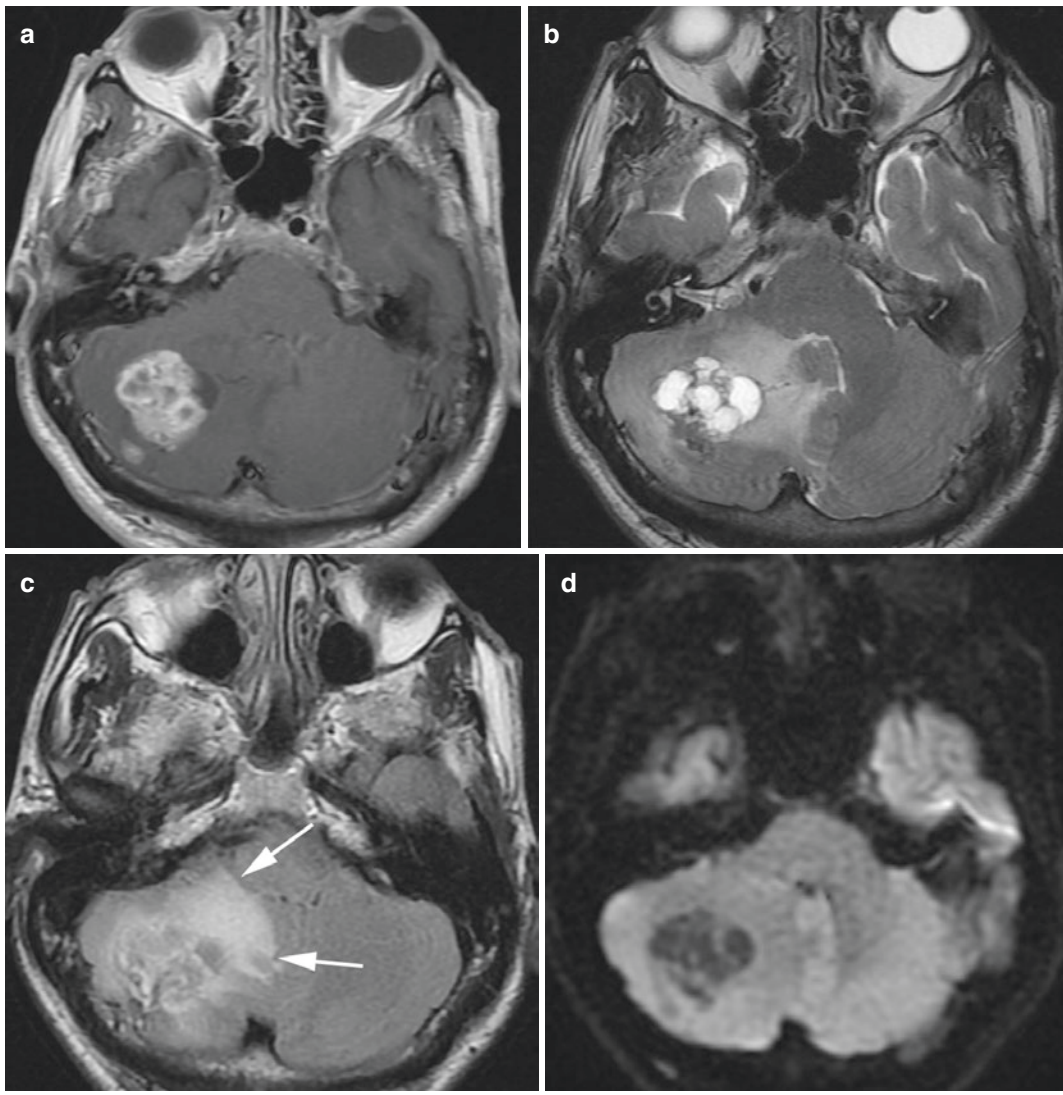

Fig. 13.14 (**a**) Axial T1-weighted contrast-enhanced MRI demonstrates an enhancing mass in the right cerebellar hemisphere. (**b**) Axial T2-weighted MRI. Multiple cystic areas are demonstrated within the mass. (**c**) Axial FLAIR MRI, white matter oedema in the periphery of the tumour (arrows) with mass effect on the fourth ventricle and secondary hydrocephalus. (**d**) Axial DWI MRI. No diffusion restriction is noted. (**e**) Susceptibility-weighted images (SWI) low signal intensity areas indicating the presence of blood products. (**f**) Axial contrast-enhanced abdominal CT, 1- basal and 2- portal phase. Multicystic pancreatic mass is shown

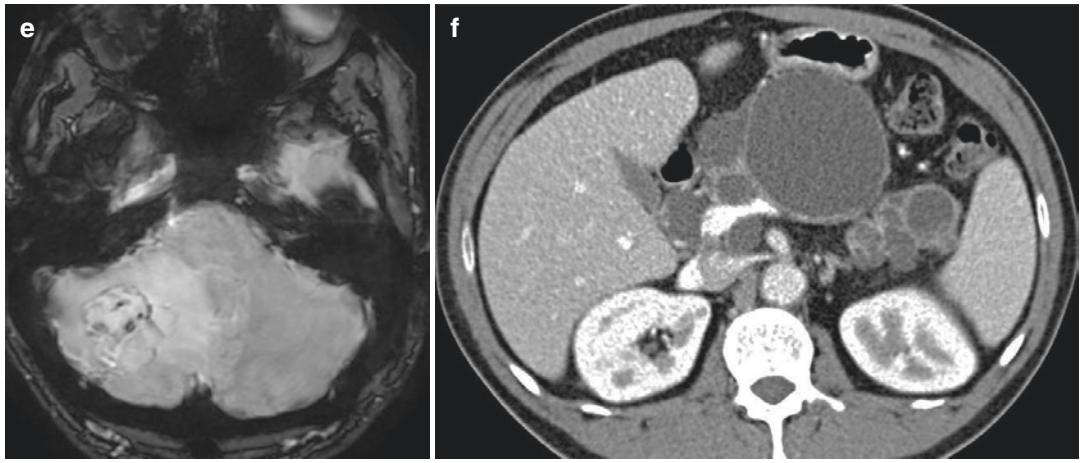

Fig. 13.14 (continued)

13.14.2 Epidemiology

Haemangioblastoma of the CNS are tumours diagnosed in young to middle aged adults. Most cases are sporadic, but younger patient tends to be related to VHL disease. Typical symptoms are related to mass effect in the posterior fossa.

13.14.3 Pathology and Genetics

Haemangioblastoma features the nodule within a cyst appearance. It is a highly vascular tumour with flow voids, sometimes, enlarged arterial feeders are demonstrated. Is suggested that the cystic component most likely arises by exudation from the solid nodule vascular component. 95% are in the posterior fossa. Usually it does not grow and has a very low Ki67 index (WHO I).

13.14.4 Clinical Management

Most patients are cured with surgical resection. In patients with very large tumours, pre-surgical embolisation makes easier the resection. Incomplete surgery is treated with RDT.

13.14.5 Imaging Findings and Differential Diagnosis

The lesion features a cystic mass with a mural nodule that vividly enhances and often has prominent flow voids. Arterial feeders may be demonstrated. Calcification is possible. Perfusion rCBV shows high ratios. The typical differential is the pilocytic astrocytoma and brain metastases.

Take-Home Messages

- Cystic mass with a peripheral enhancing nodule in the posterior fossa suspect haemangioblastoma. Differential diagnosis with unique cystic metastasis (lung, breast…)

Further Reading

1. Quadery FA, Okamoto K. Diffusion-weighted MRI of haemangioblastomas and other cerebellar tumours. Neuroradiology. 2003; 45:212–219
2. Gnanalingham KK, Apostolopoulos V, Chopra I, Mendoza N, Peterson D. Haemangioblastoma: a rare cause of a cerebellar mass in the elderly. British journal of neurosurgery. 2003; 17:461–4
3. Osborn AG, Hedlund GL, Salzman KL. Osborn's Brain E-Book. Elsevier Health Sciences; 2017 Nov 2
4. Slater A, Moore NR, Huson SM. The natural history of cerebellar hemangioblastomas in von Hippel-Lindau disease. AJNR 2003; 24:1570–1574

13.15 Case 15

13.15.1 Images and Legends

44-year-old male with altered mental status.

Biopsy was performed; the pathological diagnosis was diffuse large B-cell lymphoma. CD20+.

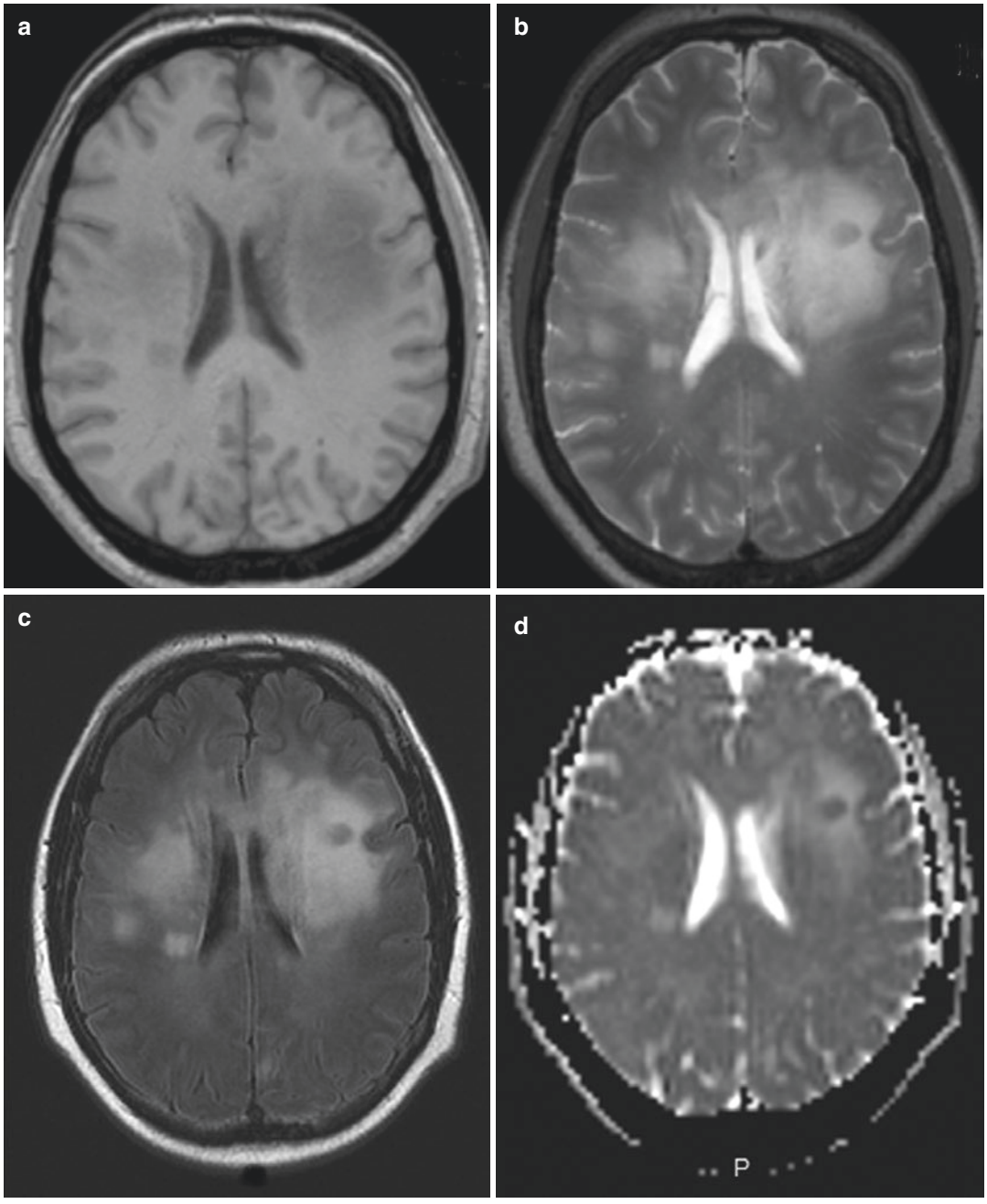

Fig. 13.15 (**a**) Axial T1WI demonstrates a hypointense subcortical left frontal lobe mass. (**b**) Axial T2WI shows subcortical WM high signal intensity with central hypointense component. (**c**) Axial FLAIR shows the same findings than T2WI. (**d**) ADC map demonstrates restricted diffusion with lower ADC values than normal brain in the central area. (**e**) PWI shows elevated rCBV in the central portion. (**f**) Contrast-enhanced axial T1-weighted MRI demonstrates several areas of enhancement. (**g**) MR spectroscopy shows increased Cho and decreased NAA and Cr values

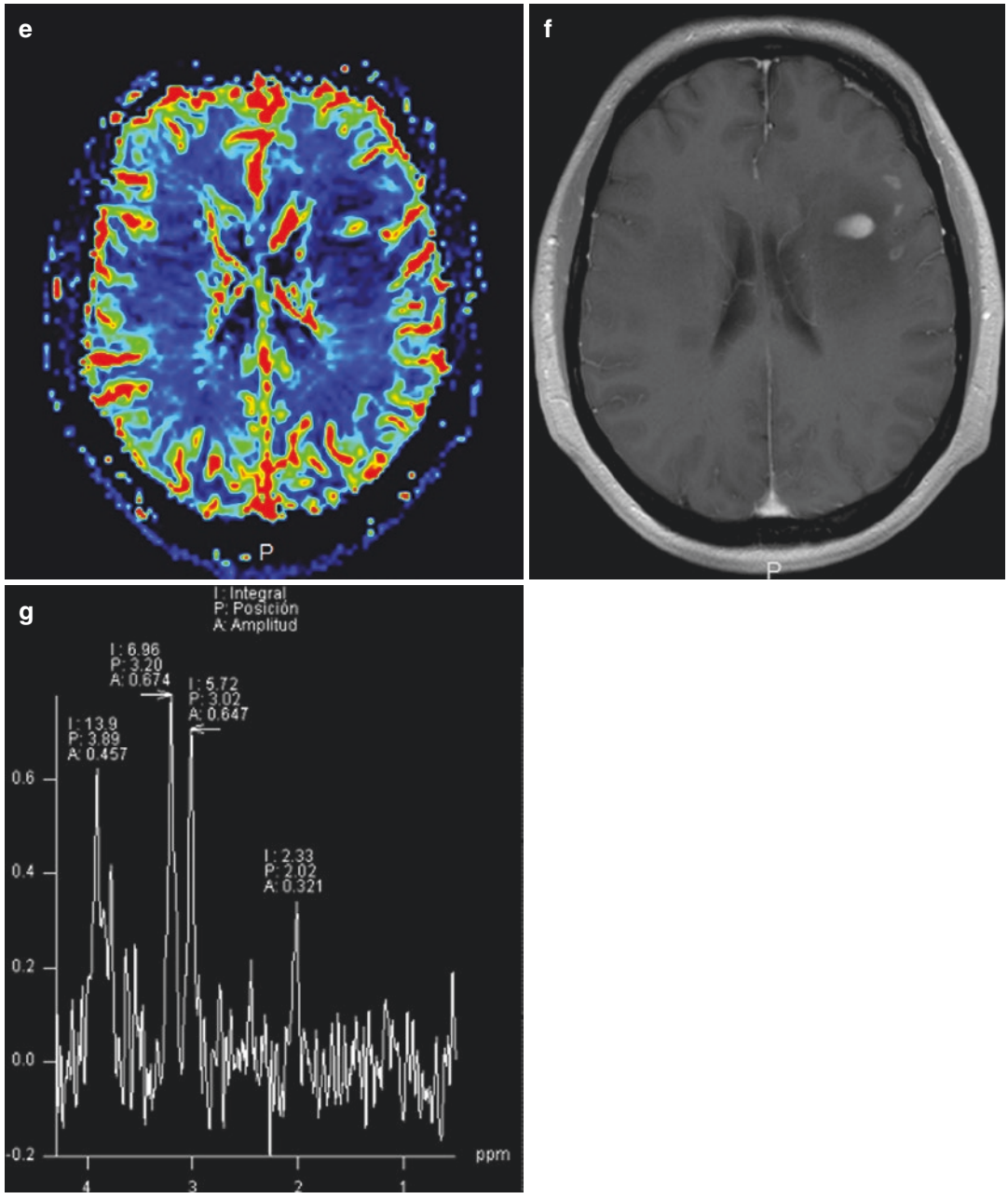

Fig. 13.15 (continued)

13.15.2 Epidemiology

Primary CNS lymphoma accounts for 1–5% of all brain tumours. The incidence rates of PCNSL are increasing among immunocompetent patients. Immunocompromised patients have an increased risk of PCNSL.

13.15.3 Pathology and Genetics

The majority (>90%) of PCNSL are B-cell tumours: diffuse large B-cell lymphoma and high-grade Burkitt-like B-cell lymphoma. Diffuse large B-cell lymphoma is the most common type

and is characterised by reactivity for CD19, CD20, CD22, CD79a and PAX-5.

13.15.4 Clinical Management

The patient was treated with steroids plus chemotherapy and radiotherapy.

These tumours are often high grade and have a poor prognosis despite treatment.

13.15.5 Imaging Findings and Differential Diagnosis

PCNSL are hypointense to grey matter in T1WI with intense homogeneous enhancement in high-grade tumours. They are usually iso-hypointense in T2WI with lower ADC values than normal brain.

Perfusion images show mild increase rCBV in enhancing areas. MR spectroscopy shows increased Cho and markedly decreased NAA and Cr values.

Differential diagnosis includes secondary CNS lymphoma, glioblastomas, cerebral toxoplasmosis, tumefactive MS and brain abscesses.

Take-Home Messages

- PCNSL are generally B-cell high-grade tumours that have a poor prognosis despite treatment
- MRI plays an important role in diagnosis and detection of treatment-related complications

Further Reading

1. Royer-Perron L, Hoang-Xuan K, Alentorn A. Primary central nervous system lymphoma. Curr Opin Neurol. 2017; 30:669–676
2. Mansour A, Qandeel M, Abdel-Razeq H, Abu Ali HA. MR imaging features of intracranial primary CNS lymphoma in immune competent patients. Cancer Imaging. 2014; 14:1–9
3. Haldorsen IS, Espeland A, Larsson EM. Central nervous system lymphoma: Characteristic findings on traditional and advanced imaging. Am J Neuroradiol. 2011; 32:984–92
4. Slone HW, Blake JJ, Shah R, Guttikonda S, Bourekas EC. CT and MRI findings of Intracranial Lymphoma. AJR 2005; 184: 1679–1685